

NASA Technical Memorandum 84568

Application of Nonlinear Adaptive Motion Washout to Transport Ground-Handling Simulation

Russell V. Parrish and Dennis J. Martin, Jr.

FEBRUARY 1983



NASA Technical Memorandum 84568

Application of Nonlinear Adaptive Motion Washout to Transport Ground-Handling Simulation

Russell V. Parrish
*Langley Research Center
Hampton, Virginia*

Dennis J. Martin, Jr.
*Sperry Systems Management
Hampton, Virginia*



National Aeronautics
and Space Administration

**Scientific and Technical
Information Branch**

1983

SUMMARY

The application of a nonlinear coordinated adaptive motion washout to the transport ground-handling environment is documented. Additions to both the aircraft math model and the motion washout system are discussed. The additions to the simulated-aircraft math model provided improved modeling fidelity for braking and reverse-thrust application, and the additions to the motion-base washout system allowed transition from the desired flight parameters to the less restrictive ground parameters of the washout.

Encountered in the process of tailoring motion cues specifically for a ground-handling environment were three notable facets. A scaling of 1.0 prior to washout for representation of negative longitudinal acceleration and a scaling of 0.5 for positive acceleration were desired by the participating pilots. The second facet was the ability to realistically represent the ground-handling environment without translational motion of the motion base in order to eliminate the objectionable hydraulic noise of the base actuators. The third facet was a fact usually recognized only by the designers of washout systems, namely, that the fidelity of motion cues are dependent in the first instance on the fidelity of the mathematical model of the aircraft providing the inputs to the cueing system.

INTRODUCTION

The increasingly prevalent use of flight simulators in lieu of actual flight operations for the purposes of training, operational studies, and research is presently being extended to the area of aircraft directional control on runways (ref. 1). While extensive effort has been expended on the modeling aspects of landing gears, skid-control braking systems, and adverse runway conditions (surface roughness, weather-induced surface conditions, runway crown, etc.), less attention has been paid to the motion-simulation aspects of the problem. It is presumed, from lack of other indications, that most ground studies have utilized the same motion conditions that were utilized for the flight phases of the simulator usage, with little consideration of the requirements imposed by the changed environment. In some cases, refinements to provide touchdown bump and runway roughness to the vertical axis cueing were probably made in the most expedient way possible.

In answer to the growing demand at the Langley Research Center for simulation of aircraft ground handling (in the area of ground guidance systems, high-speed turn-offs, and aircraft braking and steering systems), a study was undertaken to apply the highly successful nonlinear adaptive washout (refs. 2 and 3) directly to the ground-handling environment. This report documents the results of that effort, detailing the additions made to both the aircraft math model and the washout system, to provide motion cues tailored to the ground environment. No attempt is made to justify the use of motion cues in ground-handling-simulation tasks. (Ref. 4 deals with this topic.) Although the parameter values of this study pertain to a specific transport aircraft, experience has shown that because of the adaptive nature of the nonlinear washout, modifications to allow application to other vehicles would be minimal.

SYMBOLS

a_x, a_y	aircraft body-axis longitudinal and lateral acceleration at centroid location, m/sec ² (ft/sec ²)
a_z	aircraft body-axis vertical acceleration (referenced about 1g) at centroid location, m/sec ² (ft/sec ²)
\hat{a}_x, \hat{a}_y	body-axis longitudinal and lateral acceleration commands to motion simulator at centroid location, m/sec ² (ft/sec ²)
\bar{c}	mean aerodynamic chord
$f_{i,x}, f_{i,y}$	inertial-axis translational acceleration commands prior to translational washout, m/sec ² (ft/sec ²)
$f_{s,z}$	aircraft body-axis translational acceleration (referenced about 1g) at centroid location, m/sec ² (ft/sec ²)
g	gravitational constant, 9.81 m/sec ²
p, q, r	body-axis angular velocity commands to motion simulator, rad/sec
p_a, q_a, r_a	body-axis aircraft angular velocities, rad/sec
\ddot{x}, \ddot{y}	commanded inertial translational acceleration of motion simulator, m/sec ² (ft/sec ²)
ϕ, θ, ψ	commanded inertial angular position of motion simulator, rad
$\dot{\phi}, \dot{\theta}, \dot{\psi}$	commanded inertial angular velocities of motion simulator, rad/sec
$\dot{\phi}_a, \dot{\theta}_a, \dot{\psi}_a$	aircraft angular velocities, rad/sec

SIMULATOR CHARACTERISTICS

Aircraft Math Model

The aircraft mathematical model, a representation of a Boeing 737-100 aircraft, included a nonlinear data package for all flight regions, a nonlinear engine model, and nonlinear models of servos, actuators, spoiler mixers, and other associated flight hardware. The simulation of the basic airframe underwent extensive validation, including comparisons with actual aircraft response data and pilot evaluations. This simulation has been and is used extensively in simulation studies at the Langley Research Center. For the subject studies, the simulated aircraft was in the landing-approach configuration with the flight characteristics as approximated in table I. The flight control system used was the manual mode rather than other modes available, such as control wheel steering, navigation, or autoland.

Computer Implementation

The mathematical model of the aircraft and the simulation hardware drives were implemented on the Langley Flight Simulation Computing Subsystems. This system,

consisting of a Control Data CYBER 175 with the necessarily associated interface equipment, solved the programmed equations 32 times a second. The average time delay from input to output (1.5 times the sample period) was approximately 47 msec.

Simulator Cockpit

The general-purpose cockpit of the Langley Visual Motion Simulator (VMS) was configured as a transport cockpit (fig. 1). The primary instrumentation consisted of an attitude director indicator (including active flight director bars and speed bug), a vertical speed indicator, a horizontal situation indicator, an altimeter, airspeed indicators (both calibrated and true), angles of attack and sideslip meters, and a turn and bank indicator.

The control forces on the wheel, column, and rudder pedals are provided by a hydraulic system coupled with an analog computer. The system allows for the usual variable feel characteristics of stiffness, damping, backlash, Coulomb friction, breakout forces, detents, inertia, and so forth. The force gradients can also be provided by the digital computer used to solve the aircraft math model. Selection of the parameters of control loading system was included in the extensive validation process for the 737-100 flight simulator.

Visual Display

The Langley VMS is provided with an "out-the-window" virtual image system of the beam-splitter, reflective-mirror type. The system, located nominally 1.27 m (4.17 ft) from the pilot's eye, presented a nominal 48° width by 36° height field of view of a 525 TV line raster system and provided a 46° by 26° instantaneous field of view. The system supplies a color picture of unity magnification with a nominal resolution on the order of 9 minutes of arc.

The scene depicted in the virtual image system was obtained from a terrain model board. The state-of-the-art TV camera transport system used in conjunction with a sophisticated terrain model board, the Langley Visual Landing Display System (VLDS), is described in reference 5. The maximum speed capability of the system is 229 m/sec (444 knots), with vertical speed capabilities of ± 152 m/sec (± 30 000 ft/min). The translational lags of the system are 15 msec or less and the rotational lags are 22 msec or less. The average total visual delay, including computational throughput delay, was thus less than 70 msec.

Motion System

The motion performance limits of the Langley six-degree-of-freedom base are shown in figure 1. These limits are for single-degree-of-freedom operation. Conservatism must be exercised in the use of the position limits, since these limits change as the orientation of the synergistic base varies. References 6 to 8 document the characteristics of the system, which possesses time lags of less than 15 msec. Thus, the average total motion delay, including computational throughput, is less than 60 msec (ignoring the lead introduced by washout) and is quite compatible with the visual delays. The washout system used to present the motion-cue commands to the motion base is nonstandard. It was conceived and developed at the Langley Research Center, and it is documented in references 2, 3, and 9. The basis of the washout is the continuous adaptive change of parameters to (1) minimize a cost functional

through continuous steepest descent methods and (2) produce the motion cues in translational accelerations and rotational rates within the motion envelope of the synergistic base.

The major motivation for the coordination of rotational and translational motion is the fact that translational cues are induced by angular displacement of the motion base in pitch or roll. Therefore, sustained translational cues can be represented on a motion simulator by tilting the pilot and utilizing the gravity vector to present the cue. However, the tilt angle must be obtained without pilot knowledge; that is, the rotation necessary to obtain the tilt angle should be achieved with a rate below the pilot's sense threshold. Thus the initial portion of the cue, the onset, can only be represented by translational motion until the tilt angle is obtained.

In the case of a desired rotational cue, presentation of the onset cue by means of rotation alone results in a false translational cue because of temporary misalignment of the gravity vector. Thus, translational motion is required to offset the false cue induced by rotational motion. The specific parameters of the nonlinear coordinated adaptive washout used for the flight phase of this study are presented in table II. Modifications and additions to the system for the ground phase are presented in the next section of this paper.

THE NONLINEAR ADAPTIVE MOTION WASHOUT

A brief review of the application of the nonlinear adaptive motion washout (shown in block-diagram form in fig. 2) to the transport flight regime will be presented before discussion of the ground phase of motion cueing.

Flight Regime

The high degree of success of the nonlinear washout in the transport flight regime has been attributed directly to the fundamental difference between linear washout and nonlinear washout.

Fundamental difference.— Figure 3 illustrates the fundamental difference in terms of motion cues between a linear filter and a nonlinear adaptive filter for the first-order case. The difference is an anomalous rate cue presented by the linear filter as the pulse input in rate returns to zero. This false cue is most evident for pulse-type inputs and disappears as the input becomes sinusoidal. Thus, the difference between filters varies, depending upon the responsiveness of the vehicle and the pilot's input in each axis but not upon the parameter values of the filters.

Figure 4 presents a comparison of linear and nonlinear washout as applied to the 737 simulation for an aileron pulse input. As shown in figure 4, the linear washout (fig. 4(b)) represents the roll acceleration (fig. 4(a)) well, ignoring the scaling, while presenting the false cue in rotational rate. The nonlinear washout shown in figure 4(c) practically ignores the aircraft roll acceleration reversal of figure 4(a) at Time = 8 sec in order to eliminate the false rate cue. The importance of presenting the rotational rate cue properly rather than the rotational acceleration cue is documented in references 3, 10, and 11 and is illustrated in tables III and IV.

Table III reproduces the data of references 3, 10, and 11 in which the subjective opinions of seven pilots compare the motion cues produced by the linear (the

open symbols) and nonlinear (the solid symbols) washout methods under instrument conditions. The values of the parameters of each washout were chosen as the result of an attempt to optimize subjectively for the stipulated simulation (i.e., the 737-100 simulated on the visual motion simulator). The same formal evaluation process was repeated with nine pilots for motion cue ratings under the visual environment provided by the VLDS (table IV).

The pilots were asked to rate the motion cues presented by each washout method for throttle, column, wheel, and pedal inputs about a straight-and-level condition in a landing approach mode. Each pilot determined his own evaluation inputs. In addition to rating the motion for each type of control input, the pilots were asked to rate how well the overall motion came to representing that of an airplane. (Does it "feel" like an airplane?) The rating categories were excellent, good, fair, poor, and unacceptable, with additional ratings halfway between each of the given categories.

No problems were experienced with the synchronization of motion and visual cues with either washout, with the exception of the false rotational rate cues produced in roll and yaw by the linear washout method. Table IV presents the evaluation results for the washouts under visual conditions from reference 11. Again, the open symbols represent the pilot's rating of the linear method, and the solid symbols, that of the nonlinear method. The first four pilots, represented by the triangular symbols, had actual 737-100 cockpit experience.

Motion for each washout was restricted to five degrees of freedom because of the fact that extreme hydraulic noise is induced by the heave motion of the synergistic base and the fact that only a small amount of vertical cue was available. The small amount of vertical cue available is due to a combination of the position limits of the motion base and the short-period frequency of the 737 aircraft in the landing approach configuration. The cue available for heave under these conditions is less than $0.05g$ - the product of amplitude, 0.457 m (1.5 ft), and frequency squared (frequency less than 1 rad/sec). The heave axis was therefore used only to present the high-frequency turbulence cues.

Longitudinal inputs.- Under both instrument and visual conditions, very little difference was noted by the pilots for longitudinal inputs. The longitudinal characteristics of the 737 prevent pulse-type responses; and this constraint, coupled with the coordination of pitch cues with longitudinal acceleration, obscures the fundamental difference between the washout methods.

Lateral inputs.- The ratings of roll and yaw cues under visual conditions reinforce the findings of the motion-cue evaluations under instrument conditions. All pilots rated the nonlinear roll cues to be better than the linear cues. The nonlinear yaw cues were also rated higher.

Overall airplane feel.- The nonlinear washout was rated by all pilots higher than the linear washout in terms of overall airplane feel. All pilots specifically objected to anomalous rotational rate cues in roll and yaw with the linear method. Since the pilots considered roll representation to be most important in terms of overall airplane feel, the elimination of the objectionable anomalous rate cues is highly desirable.

Ground Regime

The approach taken in applying the nonlinear washout to the ground regime followed the successful approach previously utilized in transport, vertical take-off and landing (VTOL), and fighter work (refs. 12, 13, and 14, respectively), that is, to present as much of the motion cues as possible using nonlinear techniques without major concern for physiological considerations. As in the past (ref. 3), the fixed parameters of the washout system were chosen offline by an "analog matching" technique on fixed-base generated data. The body-axis translational accelerations and rotational rates of the aircraft were displayed and the motion command time histories were then compared in an iterative parameter selection process. The resulting parameters are presented in table II. Provision was made to either fair over a 0.5-sec period (during ground/air transitions) from the flight version to the ground version (or vice versa), or to instantaneously change parameters at touchdown/lift-off. The asterisk and the dagger of table II indicate faired parameters and instantaneously set parameters, respectively. An examination of typical motion cues generated by the ground version of the washout, as well as an examination of additions resulting from the subjective comments of several qualified NASA research pilots, is presented in the next section.

The subjective comments of the pilots led to additions to the aircraft mathematical model to provide increased realism to the braking characteristics and the reverse-thrust characteristics. No dynamics had been provided for either system in the simulation program, resulting in the instantaneous application of stopping force rather than a gradual buildup of force. This instantaneous application went unnoticed in fixed-base simulations involving ground handling and the same aircraft simulation program. However, the deficiencies were quite noticeable with motion cues.

One major modification to the washout system resulted from the piloted evaluation of the offline parameter selections. In all past motion work at the Langley Research Center utilizing either the linear washout of reference 15 or the nonlinear adaptive washout previously described, the scaling parameter on longitudinal acceleration, prior to washout, was set to 0.5, a value that is quite conventional (possibly universal). The value is used, not because a value of 1.0 is unobtainable or restricted by the motion demands that would be incurred by such a value but rather because the pilots consistently reject the value of 1.0 as giving too much tilt. However, in the simulation of decelerations on the ground, the participating pilots requested the increased cueing provided by a scaling of 1.0. In the instances of accelerations, however, the conventional scaling was preferred. Therefore, the final version of the washout for ground handling contains an input scaling of 0.5 when the aircraft has positive longitudinal acceleration and a scaling of 1.0 when the longitudinal acceleration is negative.

Typical time histories of the simulated aircraft responses and the resulting cueing are presented in figure 5; illustrations of the braking and reverse-thrust additions to follow utilize this scaling change. The scaling illustrated in figure 5 shows the net effect of the modification just discussed (input scaling) and the nonlinear adaptive washout effect of limiting the pitch angle in the coordination process.

One further modification was suggested by the pilots during the evaluation and was incorporated into the ground handling washout system. This modification was suggested because of the objectionable hydraulic noise induced by the increased translational motions (increased over those used in the flight regime) being commanded by the ground-handling washout system. The pilots felt that the contribution

to the translational cues presented by these large-amplitude low-frequency movements did not offset the distraction incurred in that presentation. (The typical excursions of 1 m at frequencies around or below 1 rad/sec were near perception threshold levels.) Evaluation of the system with the translational gain parameters fixed at zero confirmed that subjective impression. Consequently, only the rotational degrees of freedom were used once the aircraft had landed. This is true even for presentation of the bump at touchdown, as illustrated in figure 6. Highly realistic touchdown bumps for each of the three landing gears of the 737 are consistently possible, even with no translational motion.

CUE ANALYSIS AND PILOTED EVALUATION

The ground-handling environment to be examined in the context of motion cueing concerns those cues encountered after touchdown and/or prior to lift-off. The changes required in the math model for a more realistic braking and reverse-thrust representation will be discussed after the presentation of the modifications made prior to pilot evaluation. The modifications included the addition of a representation of runway roughness and the fairing of washout parameters from the flight value to the ground value (only done when necessary to prevent discontinuities induced from instantaneous changes).

Runway Roughness

No attempt was made to provide a sophisticated model of the runway surface with crown effects, surface conditions, etc. Instead, an implementation of the equation

$$l_R = 0.00057 \text{ m} \times \sin \left[\left(30 \frac{\text{rad}}{\text{sec}} + 0.1 \frac{\text{rad}}{\text{sec-knots}} \times \text{Groundspeed} \right) \times \text{Time} \right]$$

produced a value l_R that was added to the six actuator drive signals. Upon evaluation, the resulting velocity-dependent runway roughness was considered representative by the pilots.

Fairing of Parameters

The translational accelerations and rotational rates of an aircraft are quite limited once the aircraft is on the ground; hence, the washout system may be less restrictive. The problem of coordination of the lateral degrees of freedom is also much simplified on the ground because the motion base itself may be considered a ground "vehicle." (Alignment of the gravity vector is natural.) Reference 16 discusses the various coordination burdens for washout degrees of freedom in some detail. For a ground vehicle, including for our purposes motion bases, a negative roll angle induces a positive sway force - a condition unlike that of conventional aircraft in flight. Therefore, the lateral coordination burden is more amenable for ground operation than for flight.

Because the nonlinear adaptive washout is a dynamic process, fairing of the changes in system parameters from air to ground values was used to prevent the introduction of discontinuities. When it was possible to instantaneously change from one value to another, that mechanization was utilized.

Figure 6 illustrates typical simulated aircraft responses and the resultant motion cues produced by the system prior to touchdown, at touchdown, and following touchdown. (Runway roughness is not depicted.) Motion cues for a typical high-speed turnoff (about 60 knots) are shown in figure 7.

Problems of Braking

Piloted evaluation of the motion cues provided for the ground environment immediately revealed a problem with aircraft braking. Rotational force applied to the rudder pedals to produce the braking action resulted in a violent jerk in the surge-pitch coordinated cue. The problem was attributed to the lack of dynamics associated with the braking system, which resulted in an instantaneous application of the pilot's braking force. Time histories that illustrate the problem are presented in figure 8. The addition of a second-order low-pass filter with a damping of 0.707 and natural frequency of 4 rad/sec between the brake-pedal inputs and the landing-gear model yielded the behavior illustrated in figure 9; this resulting behavior was acceptable to the pilots. The time histories of longitudinal acceleration and pitch rate are of primary interest in this comparison.

Problems of Reverse Thrust

Piloted evaluation revealed a problem with the application of reverse thrust similar to that with the application of brakes. Figure 10 shows the effect of the instantaneous change from positive idle thrust to negative idle thrust. Figure 11 more dramatically illustrates the problem, with a change from a high positive thrust value to negative idle thrust. The thrust instantaneously changes sign, and then, as the engines spool down, thrust slowly reaches negative idle.

Therefore, dynamics, in the arbitrary form of first-order lag filters with a subjectively selected 0.2-sec time constant, were added between the throttle position inputs and the engine models to prevent the instantaneous reversal of thrust. Figures 12 and 13 show the effect of these changes on the situations depicted in figures 10 and 11. Figure 14 illustrates a typical touchdown and deceleration utilizing both reverse thrust and brakes, followed by an acceleration. The pilots found these changes to be quite acceptable.

CONCLUDING REMARKS

In the process of providing motion cues tailored specifically for a ground-handling environment, an environment that is much less demanding than the flight environment, three notable facets were encountered. The 1.0 scaling desired by the pilots for representation of negative longitudinal acceleration, as opposed to the traditional 0.5 desired for positive acceleration, came as a complete surprise to all persons involved in the process.

The second facet dealt with the nonuse of translational motion once the aircraft had landed. The participating pilots collectively felt that the rotational degrees of freedom supplied the necessary cues without the distracting hydraulic noise incurred with the translational motion, which provided, they felt, little additional cueing information.

The third facet, concerning the necessity of modifying the modeling of the braking and reverse thrust system, came as no surprise in the sense that the fidelity of motion cues is dependent in the first instance on the fidelity of the mathematical model providing the inputs to the cueing system.

Langley Research Center
National Aeronautics and Space Administration
Hampton, VA 23665
January 5, 1983

REFERENCES

1. Kibbee, G. W.: Expansion of Flight Simulator Capability for Study and Solution of Aircraft Directional Control Problems on Runways. NASA CR-2970, 1978.
2. Parrish, Russell V.; Dieudonne, James E.; Bowles, Roland L.; and Martin, Dennis J., Jr.: Coordinated Adaptive Washout for Motion Simulators. J. Aircr., vol. 12, no. 1, Jan. 1975, pp. 44-50.
3. Parrish, Russell V.; and Martin, Dennis J., Jr.: Comparison of a Linear and a Nonlinear Washout for Motion Simulators Utilizing Objective and Subjective Data From CTOL Transport Landing Approaches. NASA TN D-8157, 1976.
4. Parrish, Russell V.; McKissick, Burnell T.; and Steinmetz, George G.: Application of Modified Profile Analysis to Function Testing of the Motion/No-Motion Issue in an Aircraft Ground-Handling Simulation. NASA TP-1540, 1979.
5. Rollins, John D.: Description and Performance of the Langley Visual Landing Display System. NASA TM-78742, 1978.
6. Parrish, Russell V.; Dieudonne, James E.; Martin, Dennis J., Jr.; and Copeland, James L.: Compensation Based on Linearized Analysis for a Six-Degree-of-Freedom Motion Simulator. NASA TN D-7349, 1973.
7. Dieudonne, James E.; Parrish, Russell V.; and Bardusch, Richard E.: An Actuator Extension Transformation for a Motion Simulator and an Inverse Transformation Applying Newton-Raphson's Method. NASA TN D-7067, 1972.
8. Parrish, Russell V.; Dieudonne, James E.; and Martin, Dennis J., Jr.: Motion Software for a Synergistic Six-Degree-of-Freedom Motion Base. NASA TN D-7350, 1973.
9. Martin, D. J., Jr.: A Digital Program for Motion Washout on Langley's Six-Degree-of-Freedom Motion Simulator. NASA CR-145219, 1977.
10. Parrish, R. V.; and Martin, D. J., Jr.: Empirical Comparison of a Linear and a Nonlinear Washout for Motion Simulators. AIAA Paper No. 75-106, Jan. 1975.
11. Parrish, R. V.; Rollins, J. D.; and Martin, Dennis J., Jr.: Visual/Motion Simulation of CTOL Flare and Touchdown Comparing Data Obtained From Two Model Board Display Systems. AIAA Paper 76-1709, Apr. 1976.
12. Parrish, Russell V.; Houck, Jacob E.; and Martin, Dennis J., Jr.: Empirical Comparison of a Fixed-Base and a Moving-Base Simulation of a Helicopter Engaged in Visually Conducted Slalom Runs. NASA TN D-8424, 1977.
13. Ricard, G. L.; Parrish, R. V.; Ashworth, B. R.; and Wells, M. D.: The Effects of Various Fidelity Factors on Simulated Helicopter Hover. NAVTRAEQUIPCEN IH-321, U.S. Navy, Jan. 1981. (Available from DTIC as AD A102 028.)
14. Parrish, R. V.: Platform Motion for Fighter Simulations - Let's Be Realistic. A Collection of Technical Papers - AIAA Flight Simulation Technologies Conference, Sept. 1978, pp. 21-31. (Available as AIAA Paper No. 78-1574.)

15. Parrish, Russell V.; and Martin, Dennis J., Jr.: Evaluation of a Linear Washout for Simulator Motion Cue Presentation During Landing Approach. NASA TN D-8036, 1975.
16. Parrish, Russell V.; Dieudonne, James E.; Martin, Dennis J.; and Bowles, Roland L.: Coordinated Adaptive Filters for Motion Simulators. Proceedings of the 1973 Summer Computer Simulation Conference, Simulation Councils, Inc., c.1973, pp. 295-300.

TABLE I.- LINEAR APPROXIMATION OF THE FLIGHT CHARACTERISTICS OF
THE 737-100 AIRPLANE

Weight, N (lb)	400 340 (90 000)
Center of gravity	0.31 \bar{c}
Flap deflection, deg	40
Landing gear	Down
Damping ratio for -	
Short period	0.562
Long period	0.089
Dutch roll	0.039
Period, sec, for -	
Short period	6.30
Long period	44.3
Dutch roll	5.12

TABLE II.- WASHOUT PARAMETERS

Parameter	Flight version	Ground version after pilot evaluation
Components of vector from aircraft center of gravity to motion-base centroid:		
R_x , m	12.192	12.192
R_y , m	0.2286	0.2286
R_z , m	1.7399	1.7399
Longitudinal breakpoint, x_1 , m/sec ²	3.6576	*2.4384
Longitudinal scale factor, $S_{x,o}$	0.5	{ 0.5 ($a_x \geq 0$) *1.0 ($a_x < 0$)
Lateral breakpoint, y_1 , m/sec ²	2.4384	2.4384
Lateral scale factor, $S_{y,o}$	0.5	0.5
Vertical breakpoint, z_1 , m/sec ²	1.2192	†4.5720
Vertical scale factor, $S_{z,o}$	0.5	0.5
Roll breakpoint, p_1 , rad/sec	0.18	0.18
Roll scale factor, $S_{p,o}$	1.0	1.0
Pitch breakpoint, q_1 , rad/sec	0.5	0.5
Pitch scale factor, $S_{q,o}$	1.0	1.0
Yaw breakpoint, r_1 , rad/sec	0.15	0.15
Yaw scale factor, $S_{r,o}$	1.0	1.0
Pitch rate weight, W_x , m ² /rad ² -sec ²	0.00929	0.00929
Longitudinal position penalty, b_x , sec ⁻⁴	0.01	0.01
Longitudinal velocity penalty, c_x , sec ⁻²	0.2	0.2
Longitudinal damping, d_x , rad/sec	0.707	0.707
Longitudinal frequency, e_x , rad/sec ²	0.25	0.25
Longitudinal coordination gain, γ_x , rad-sec/m	0.164	*0.56
Longitudinal gains:		
$K_{\lambda,x}$, sec ³ /m ²	0.517	*3.22917
$K_{\delta,x}$, sec ³ /m ²	0.010764	0.010764
Longitudinal gains on initial parameters:		
$K_{i,\lambda,x}$, sec ⁻¹	0.02	*0.1
$K_{i,\delta,x}$, sec ⁻¹	0.5	0.5
Limits on longitudinal variables:		
$\lambda_{x,MIN}$	-0.1	-0.1
$\lambda_{x,MAX}$	1.0	†1.0
$\delta_{x,MIN}$	0	0
$\delta_{x,MAX}$	1.0	1.0
$\lambda_{x,MIN}$	-0.06	*-0.1
$\delta_{x,MIN}$	-1000	-1000

See footnotes at end of table, p. 15.

TABLE II.- Continued

Parameter	Flight version	Ground version after pilot evaluation
Initial conditions:		
$\lambda_x(o)$	1.0	[†] 1.0
$\delta_x(o)$	0.5	0.5
Roll rate weight, w_y , m^2/rad^2-sec^2	0.00929	0.00929
Lateral position penalty, b_y , sec^{-4}	0.1	*0.01
Lateral velocity penalty, c_y , sec^{-2}	2.0	*0.2
Lateral damping, d_y , rad/sec	1.2727	[†] 0.707
Lateral frequency, e_y , rad/sec^2	0.81	[†] 0.25
Lateral coordination gain, γ_y , $rad-sec/m$	0.0328	*0.0656
Lateral gains:		
$K_{\lambda,y}$, sec^3/m^2	0.517	*3.2292
$K_{\delta,y}$, sec^3/m^2	0.269098	0.269098
Lateral gains on initial parameters:		
$K_{i,\lambda,y}$, sec^{-1}	0.05	*0.1
$K_{i,\delta,y}$, sec^{-1}	1.5	1.5
Limits on lateral variables:		
$\lambda_{y,MIN}$	-0.1	-0.1
$\lambda_{y,MAX}$	0.2	[†] 0.4
$\delta_{y,MIN}$	0	0
$\delta_{y,MAX}$	0.3	0.3
$\dot{\lambda}_{y,MIN}$	-0.06	*-0.1
$\dot{\delta}_{y,MIN}$	-0.04	[†] -0.04
Initial conditions:		
$\lambda_y(o)$	0.2	[†] 0.4
$\delta_y(o)$	0.3	0.3
Vertical position penalty, b_z , sec^{-4}	0.1	0.1
Vertical velocity penalty, c_z , sec^{-2}	0.1	0.1
Vertical damping, d_z , rad/sec	1.2727	1.2727
Vertical frequency, e_z , rad/sec^2	0.81	0.81
Vertical gain, $K_{\eta,z}$, sec^3/m^2	0.516668	0.516668
Vertical gain on initial parameter, $K_{i,\eta,z}$, sec^{-1}	0.05	0.05

See footnotes at end of table, p. 15.

TABLE II.- Concluded

Parameter	Flight version	Ground version after pilot evaluation
Limits on vertical variables:		
$\eta_{z,MIN}$	0	0
$\eta_{z,MAX}$	0.25	[†] 0.5
$\dot{\eta}_{z,MIN}$	-0.06	-0.06
Initial condition, $\eta_z(o)$	0.25	[†] 0.5
Yaw position penalty, b_ψ , sec^{-4}	1.0	1.0
Yaw time constant, e_ψ , rad/sec^2	0.3	0.3
Yaw gain, $K_{\eta,\psi}$, sec/rad^2	100	100
Yaw gain on initial parameter, $K_{i,\eta,\psi}$, sec^{-1}	0.1	0.1
Limits on yaw variables:		
$\eta_{\psi,MIN}$	0	0
$\eta_{\psi,MAX}$	1.0	1.0
$\dot{\eta}_{\psi,MIN}$	-0.4	-0.4
Initial condition, $\eta_\psi(o)$	1.0	1.0
Lead compensation parameters:		
$C_{x,A}$, sec^2	0.0069	0.0069
$C_{y,A}$, sec^2	0.0069	0.0069
$C_{z,A}$, sec^2	0.0069	0.0069
$C_{x,v}$, sec	0.15	0.15
$C_{y,v}$, sec	0.15	0.15
$C_{z,v}$, sec	0.133	0.133
C_ψ , sec	0.12	0.12
C_θ , sec	0.12	0.12
C_ϕ , sec	0.12	0.12
Gravitational constant, g , m/sec^2	9.81	9.81
Program step size, h , sec	0.03125	0.03125

*Faired parameter.

[†]Instantaneously set parameter.

TABLE III.- PILOT RATINGS OF MOTION CUES FOR THE
LINEAR AND NONLINEAR WASHOUT METHODS
UNDER INSTRUMENT CONDITIONS

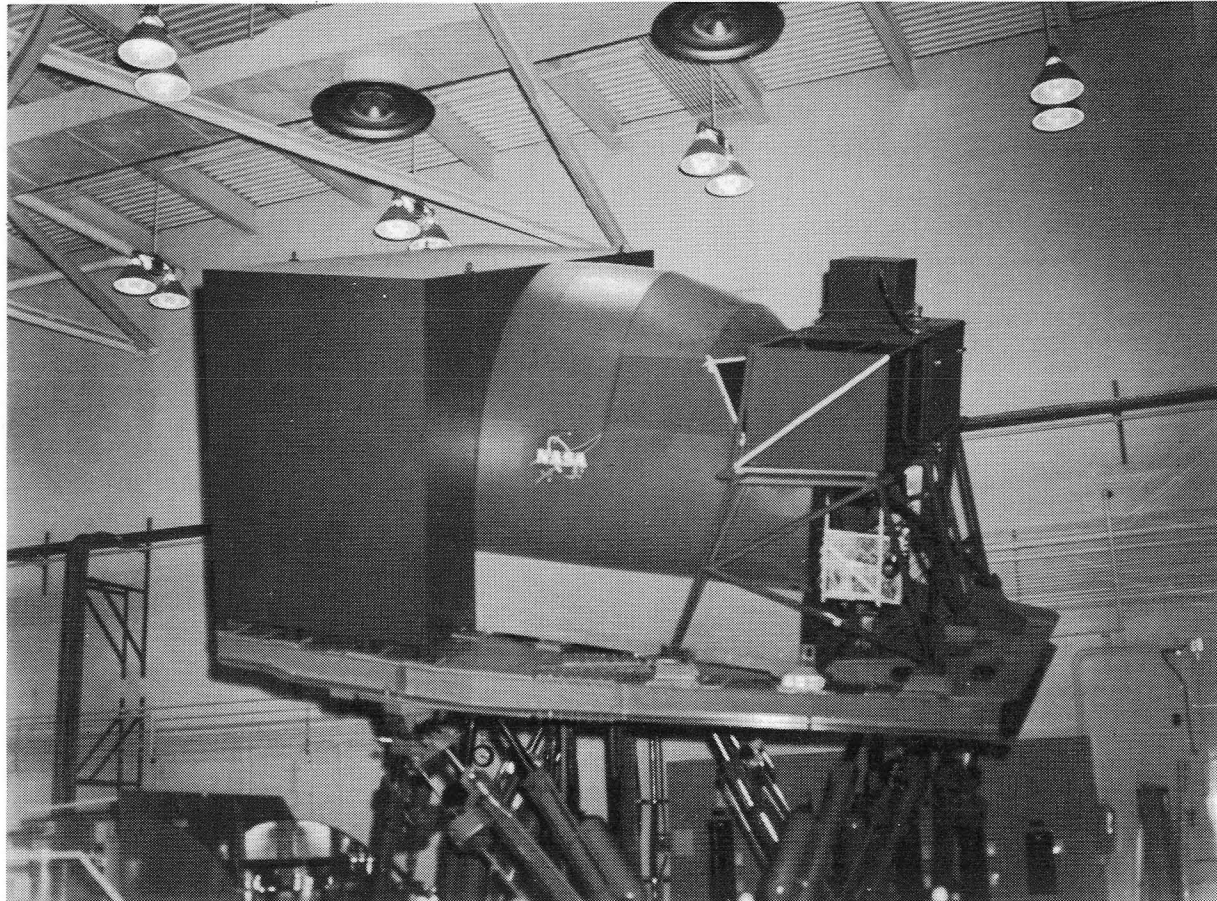
RATING INPUT		EXCELLENT	HALF- WAY	GOOD	HALF- WAY	FAIR	HALF- WAY	POOR	HALF- WAY	UNACCEPTABLE
THROTTLE				▷▷△○○□ ▷△▽●●■		◁ ◁				
COLUMN		△ ▲	○ ◁ ●	▷▽ ◁▷▽●■	○	□				
WHEEL AND PEDAL	ROLL	●	▷▷△△▽	■	▷	◁ ○		△▽○○□		
	YAW		▽ ●	▷▷△△●■	○	◁ ▽		▷△○○□		
OVERALL AIRPLANE FEEL		●	▷▷△△	▽●■	○	▷ ◁	○	△▽□		

PILOT	LINEAR WASHOUT	NONLINEAR WASHOUT	
1	△	▲	} 737 COCKPIT EXPERIENCE
2	▽	▼	
3	▷	▶	
4	◁	◀	
5	□	■	
6	○	●	
7	○	●	

TABLE IV.- PILOT RATING OF MOTION CUES FOR THE
LINEAR AND NONLINEAR WASHOUT METHODS
UNDER VISUAL CONDITIONS

RATING INPUT		EXCELLENT	HALF- WAY	GOOD	HALF- WAY	FAIR	HALF- WAY	POOR	HALF- WAY	UNACCEPTABLE
THROTTLE		◆	△ □ ▲ ■	○○○ ●●●	▽ ◁	▷ ◇				
COLUMN			△ □ ▲ ■	◁▷○○ ●●●	◇					
WHEEL AND PEDAL	ROLL	◆	△▽◀●●	●●●		△▽◁	◇ ○	○○○		▷
	YAW		◁△▲▽●●	●●●		○○◇	▽◁◇	△□		▷
OVERALL AIRPLANE FEEL			△◀◆▽●●	●●●		▽△○○	○○◇			▷

PILOT	LINEAR WASHOUT	NONLINEAR WASHOUT	
1	△	▲	} 737 COCKPIT EXPERIENCE
2	▽	▼	
3	▷	▶	
4	◁	◀	
5	□	■	
6	○	●	
7	○	●	
8	◇	◆	
9	◇	◆	



	Position	Velocity	Acceleration
Pitch	+30, -20°	±15 deg/sec	±50 deg/sec ²
Roll	±22°	±15 deg/sec	±50 deg/sec ²
Yaw	±32°	±15 deg/sec	±50 deg/sec ²
Vertical	+0.762, -0.991 m	±0.610 m/sec	±0.6g
Lateral	±1.219 m	±0.610 m/sec	±0.6g
Longitudinal	+1.245, -1.219 m	±0.610 m/sec	±0.6g

L-79-312

Figure 1.- Motion performance limits of the visual motion simulator.

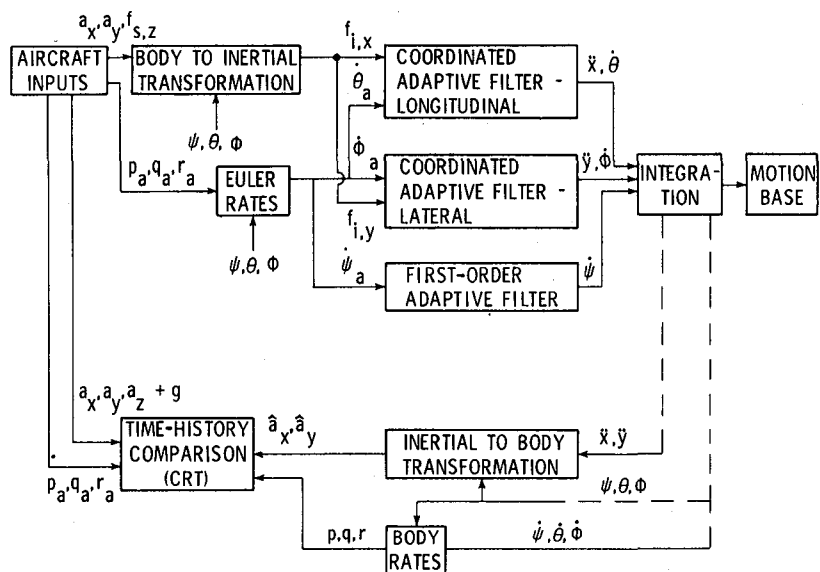


Figure 2.- Block diagram of coordinated adaptive washout.

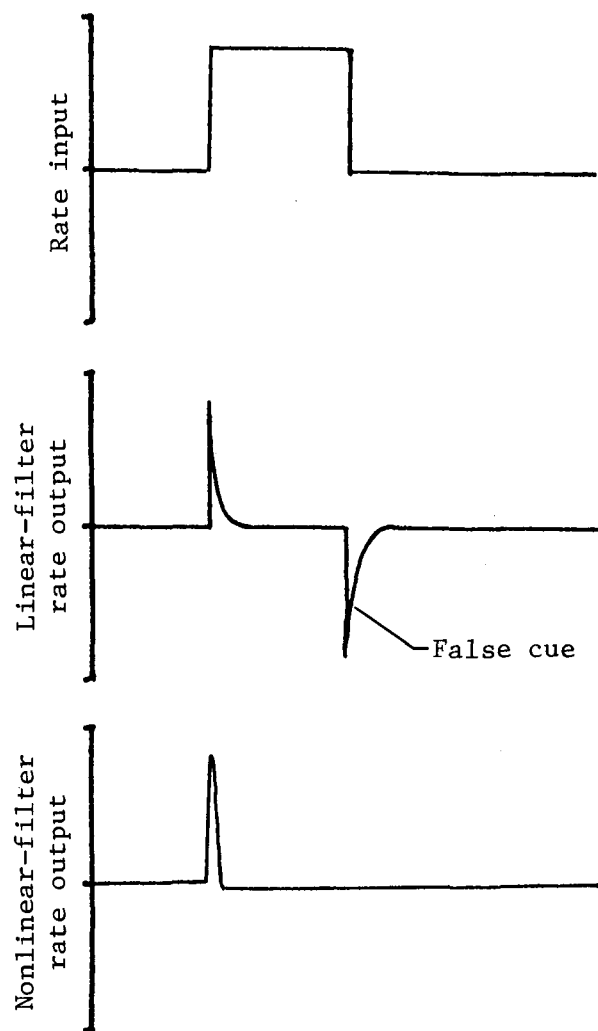
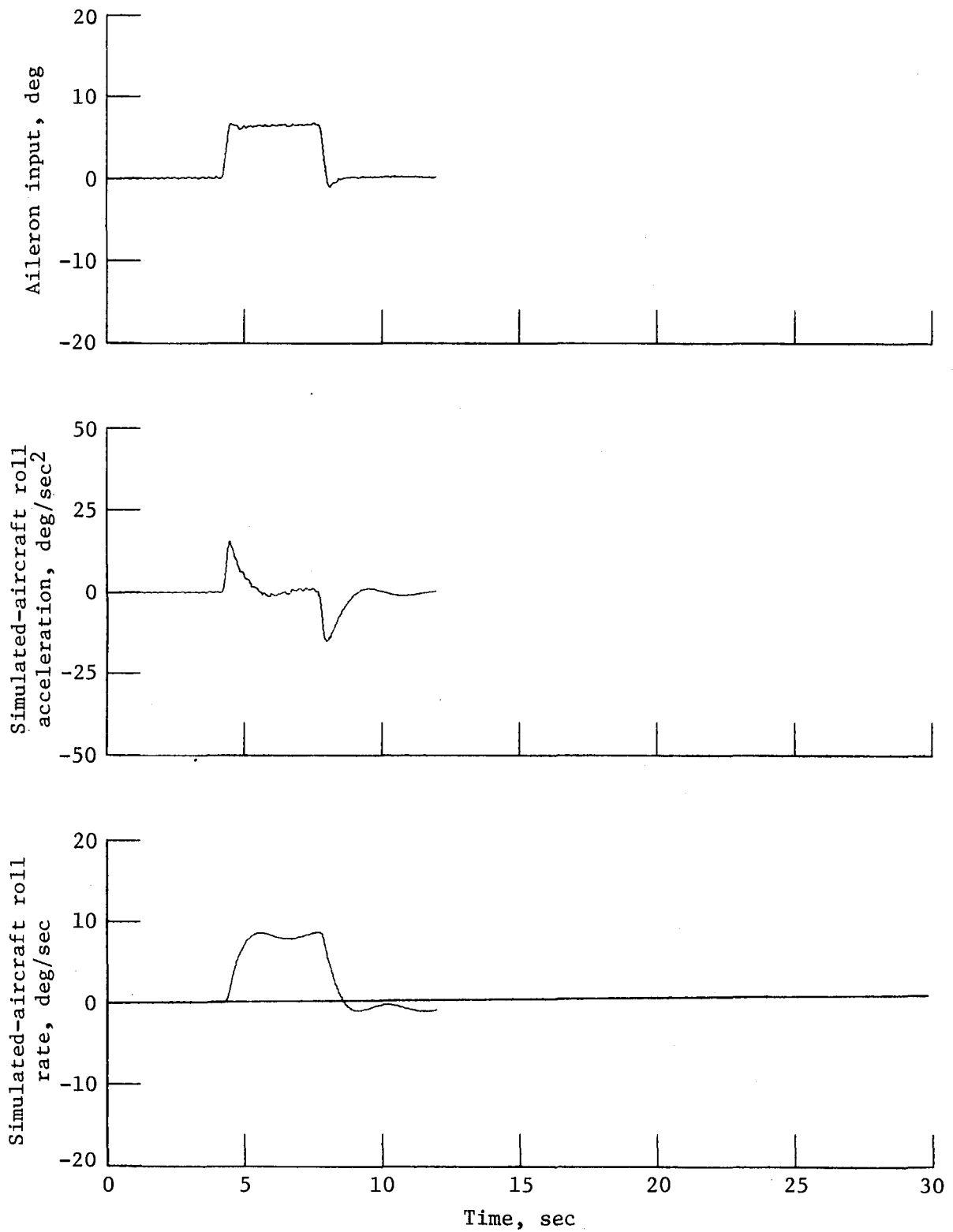
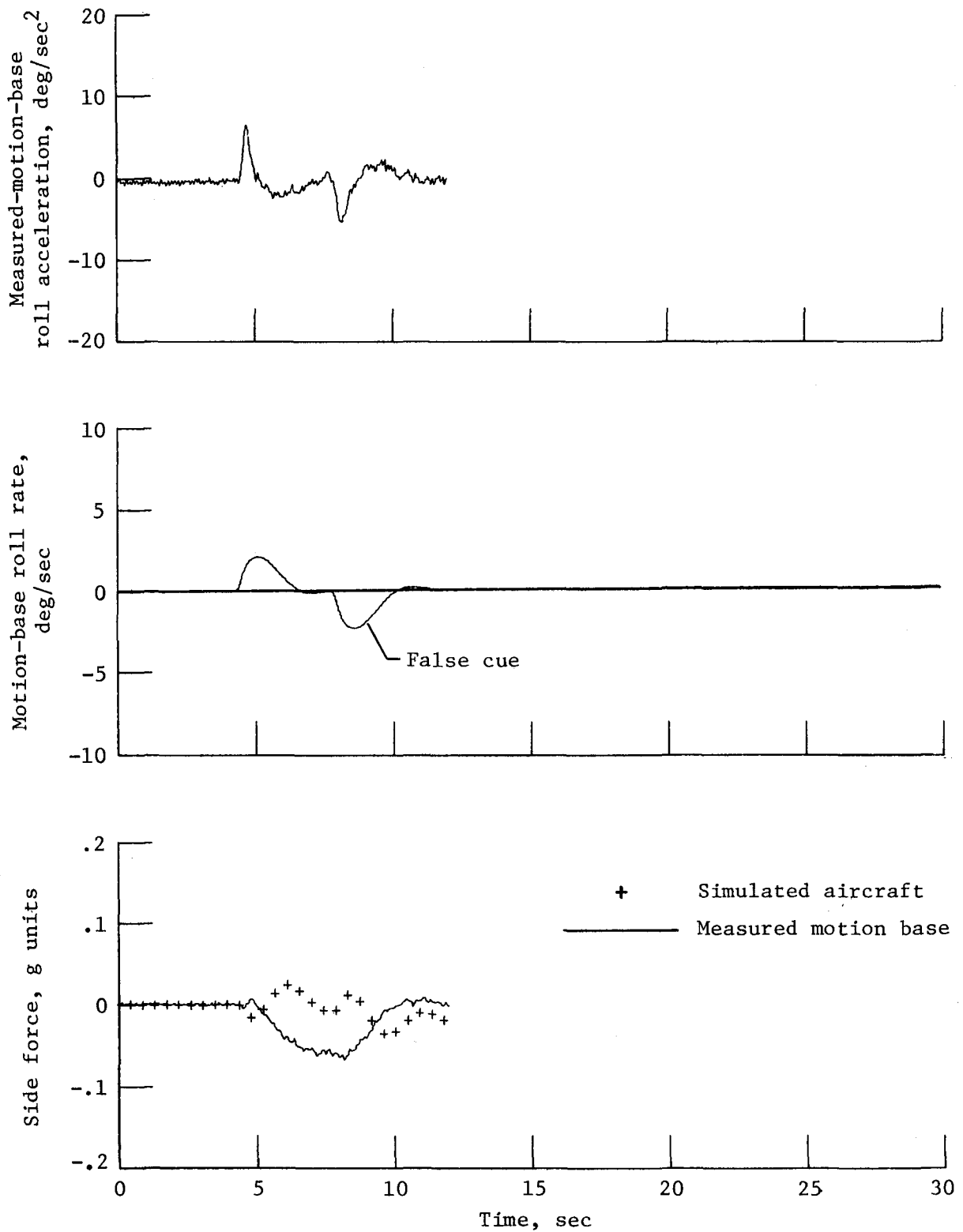


Figure 3.- Response of first-order linear and nonlinear filters to a pulse input.



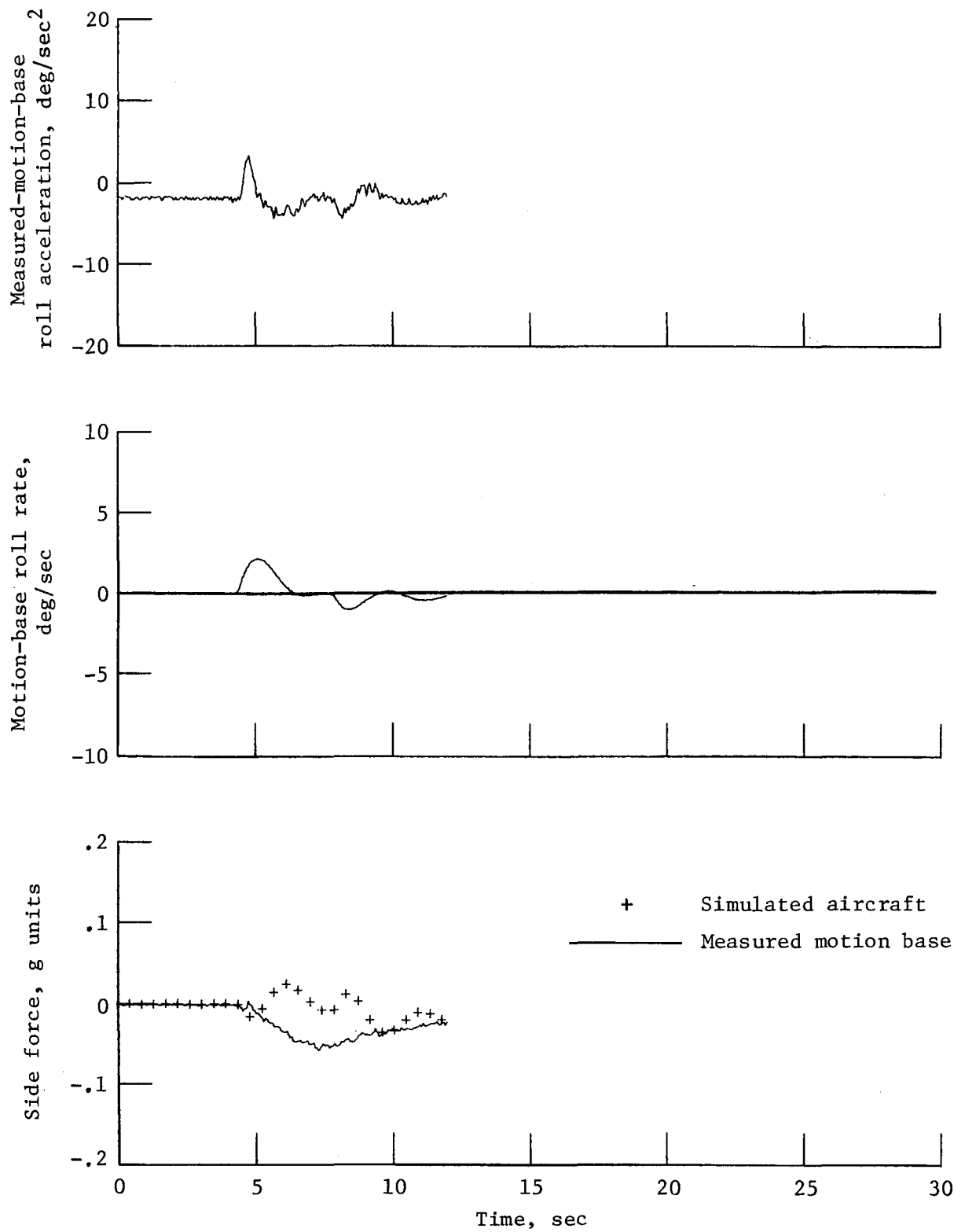
(a) 737 response.

Figure 4.- Time histories for an aileron pulse input.



(b) Linear-washout response.

Figure 4.- Continued.



(c) Nonlinear-washout response.

Figure 4.- Concluded.

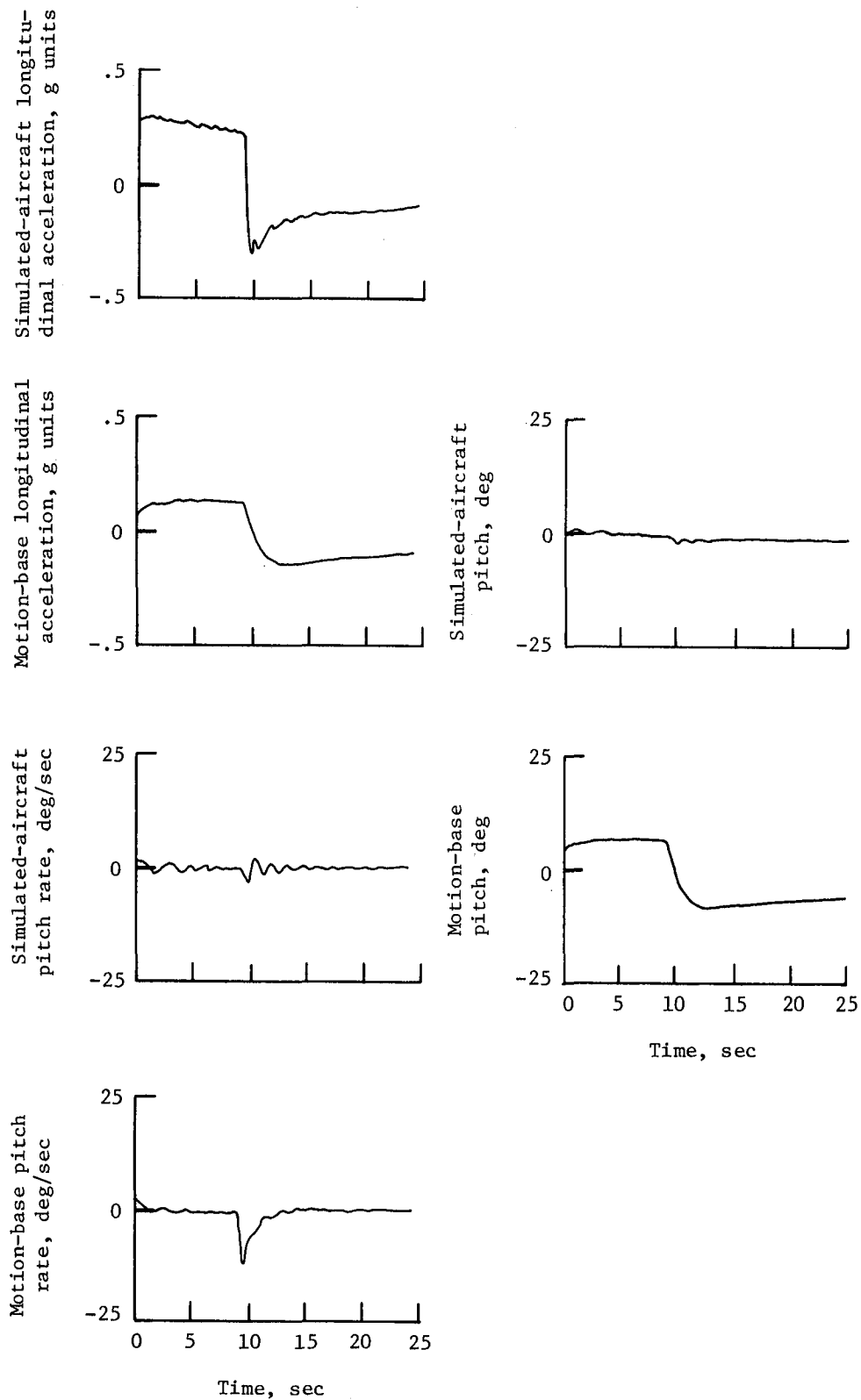
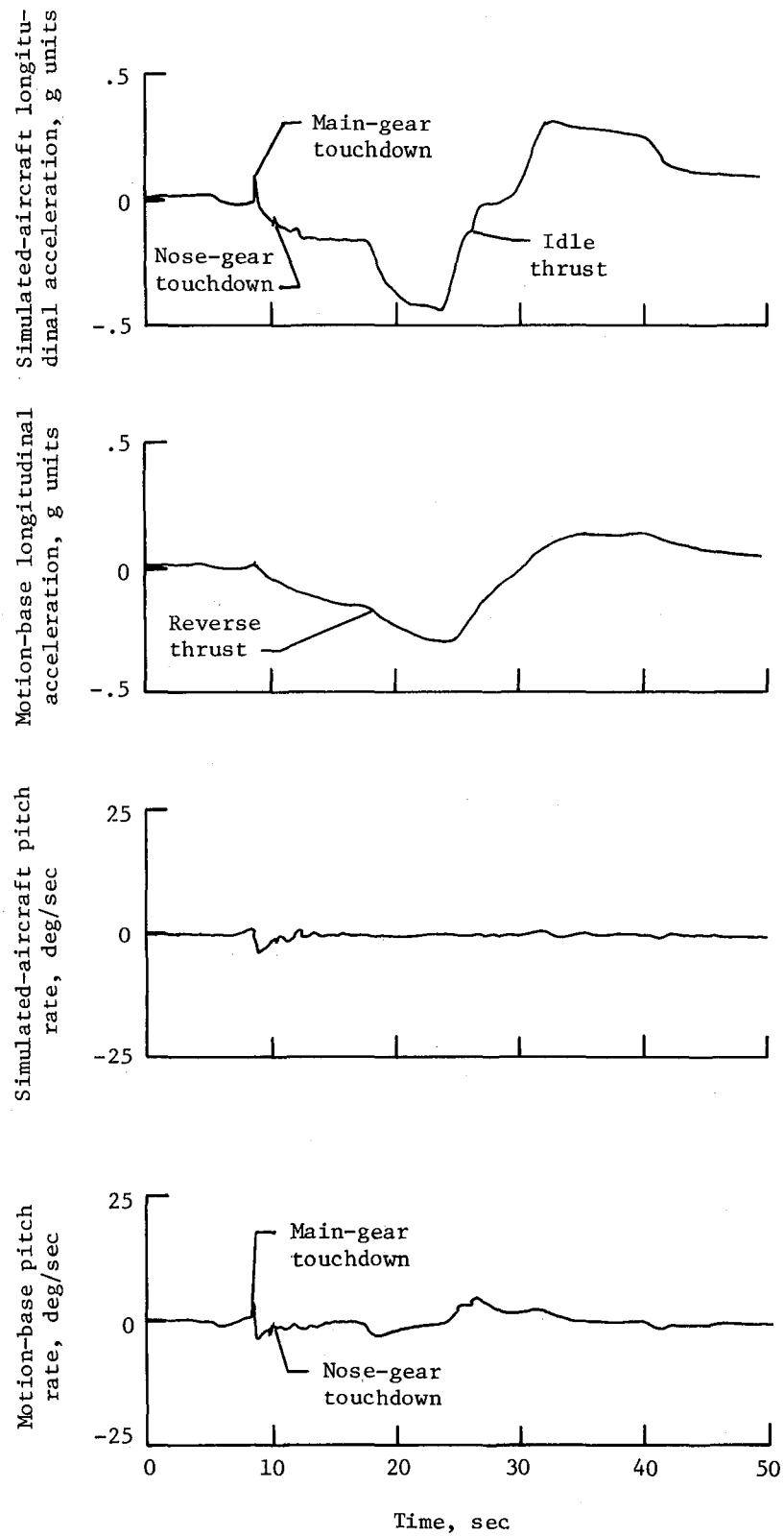
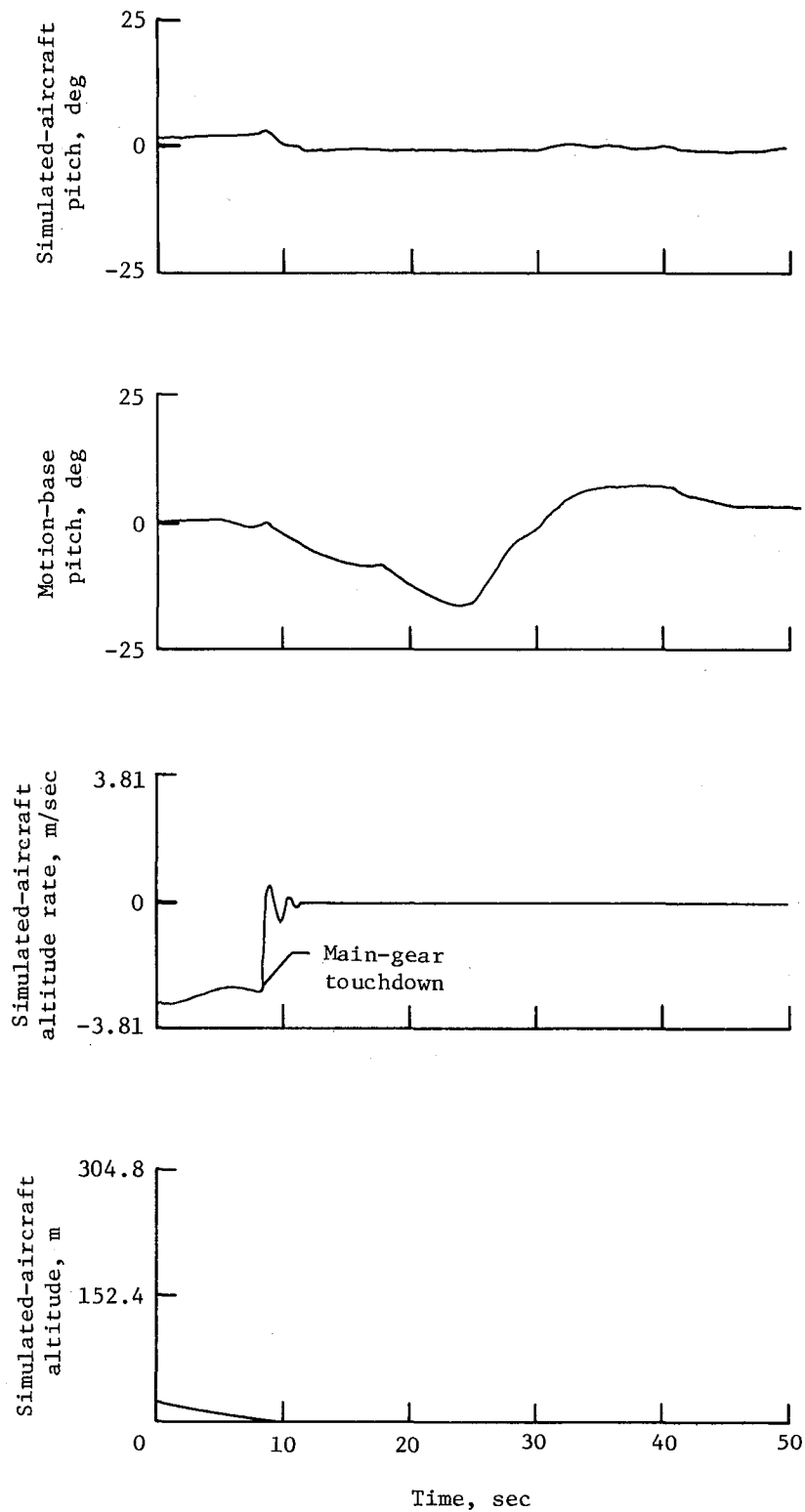


Figure 5.- Typical time histories illustrating the scaling of longitudinal acceleration for a thrust change.



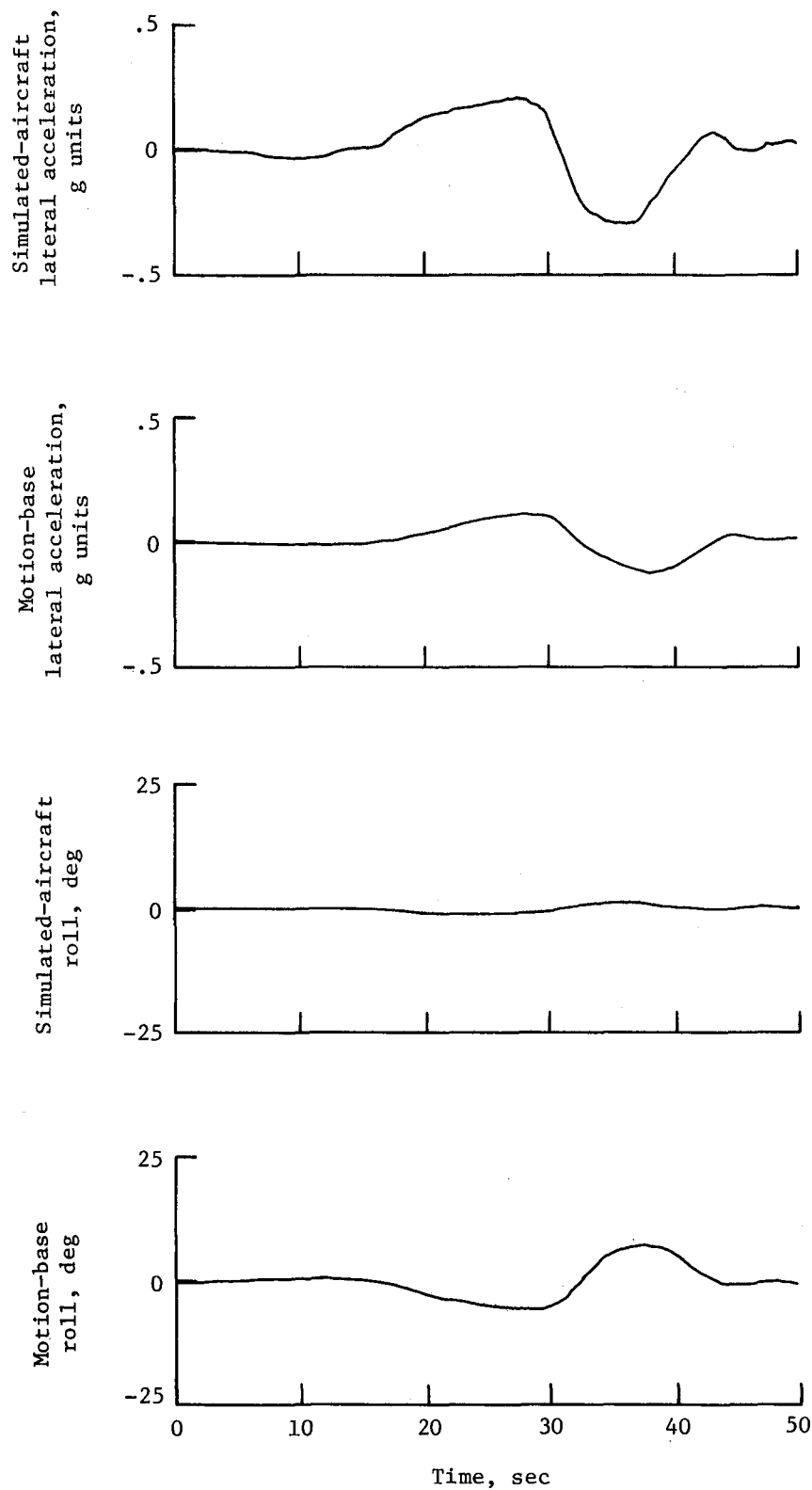
(a) Longitudinal accelerations and pitch rates.

Figure 6.- Typical time histories illustrating touchdown bumps.



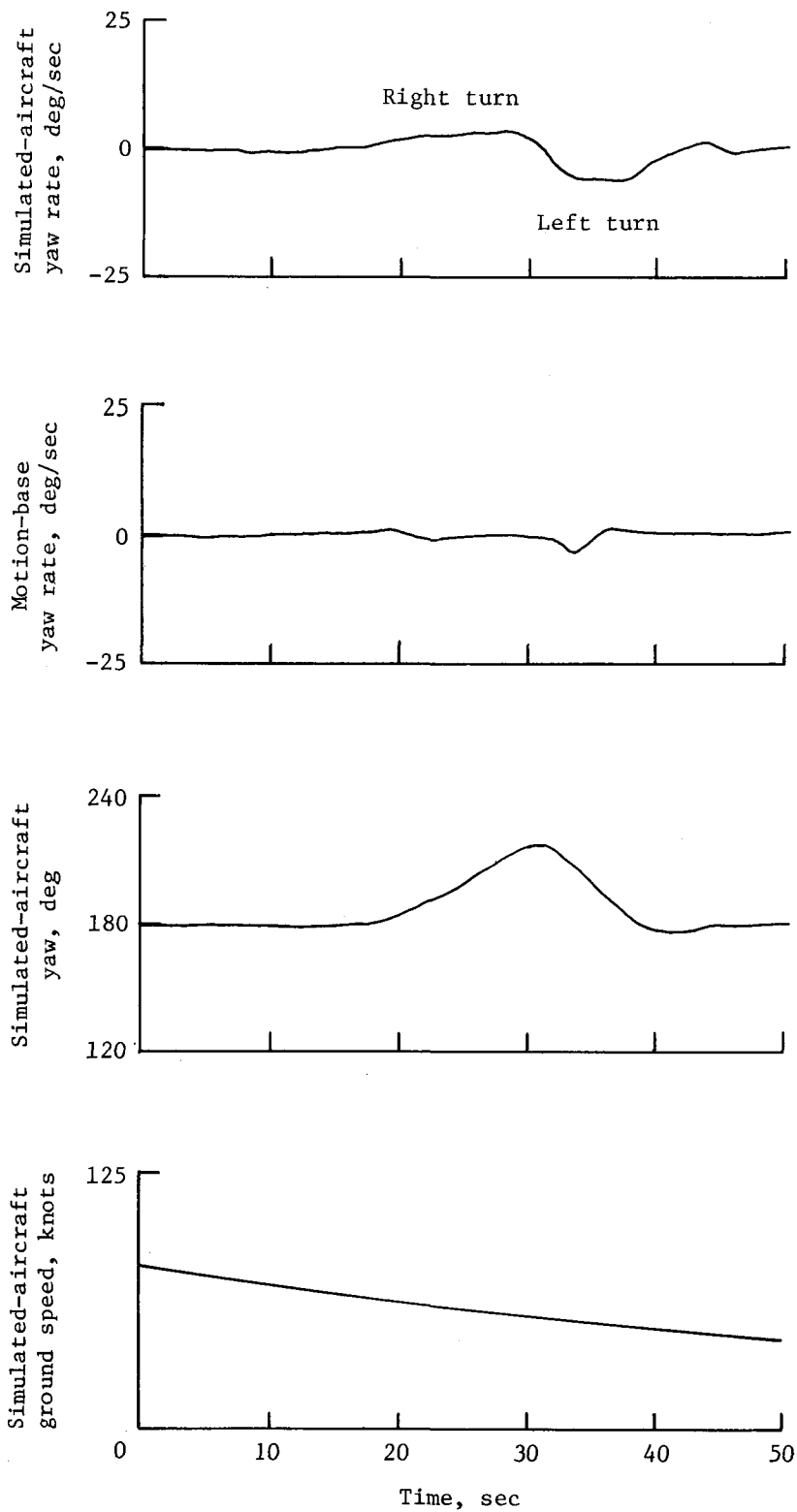
(b) Pitch angles, altitude, and altitude rate.

Figure 6.- Concluded.



(a) Lateral accelerations and roll angles.

Figure 7.- Time histories illustrating a typical high-speed turnoff.



(b) Yaw rates, yaw angle, and ground speed.

Figure 7.- Concluded.

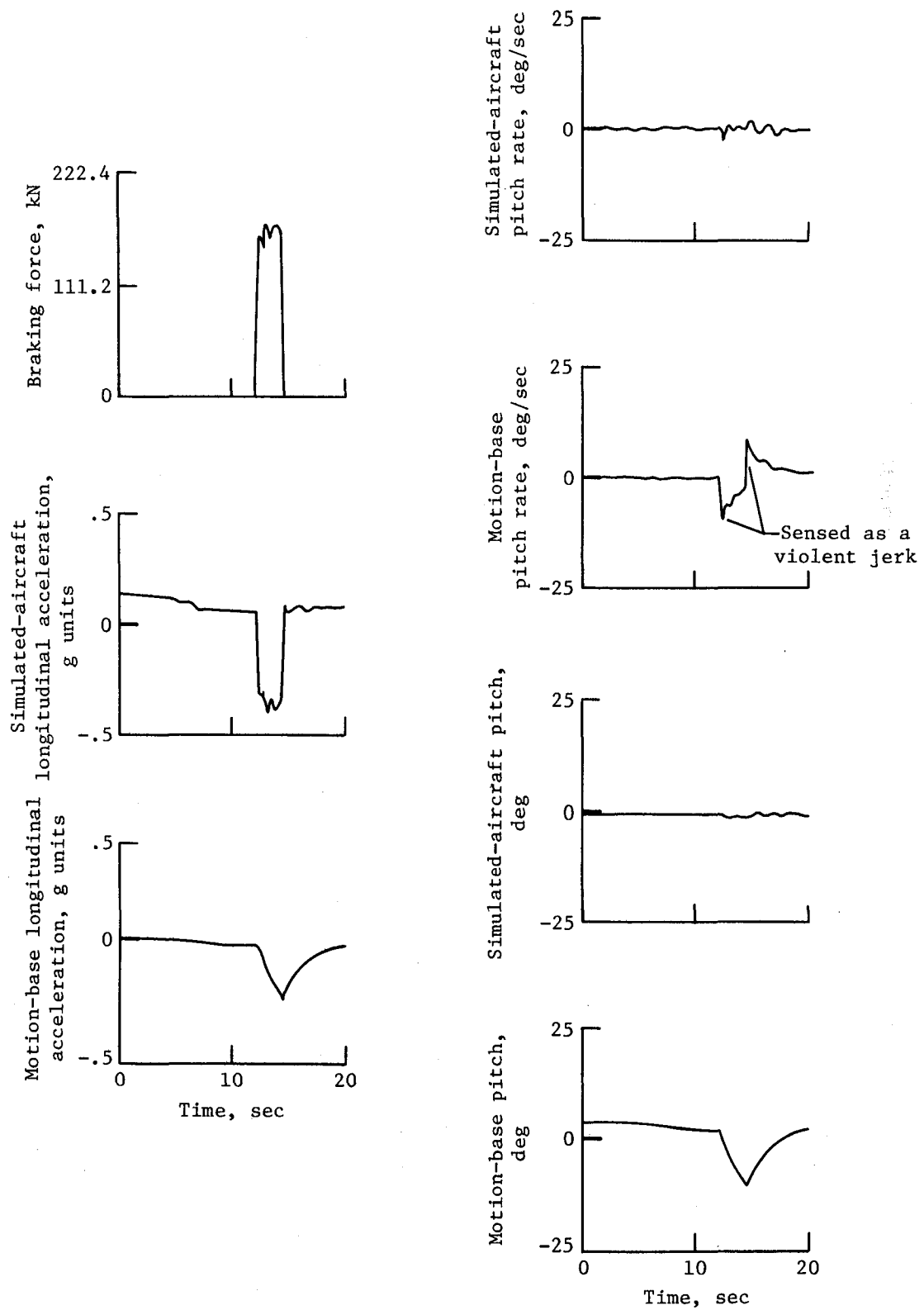


Figure 8.- Illustrations of instantaneous braking-force application.

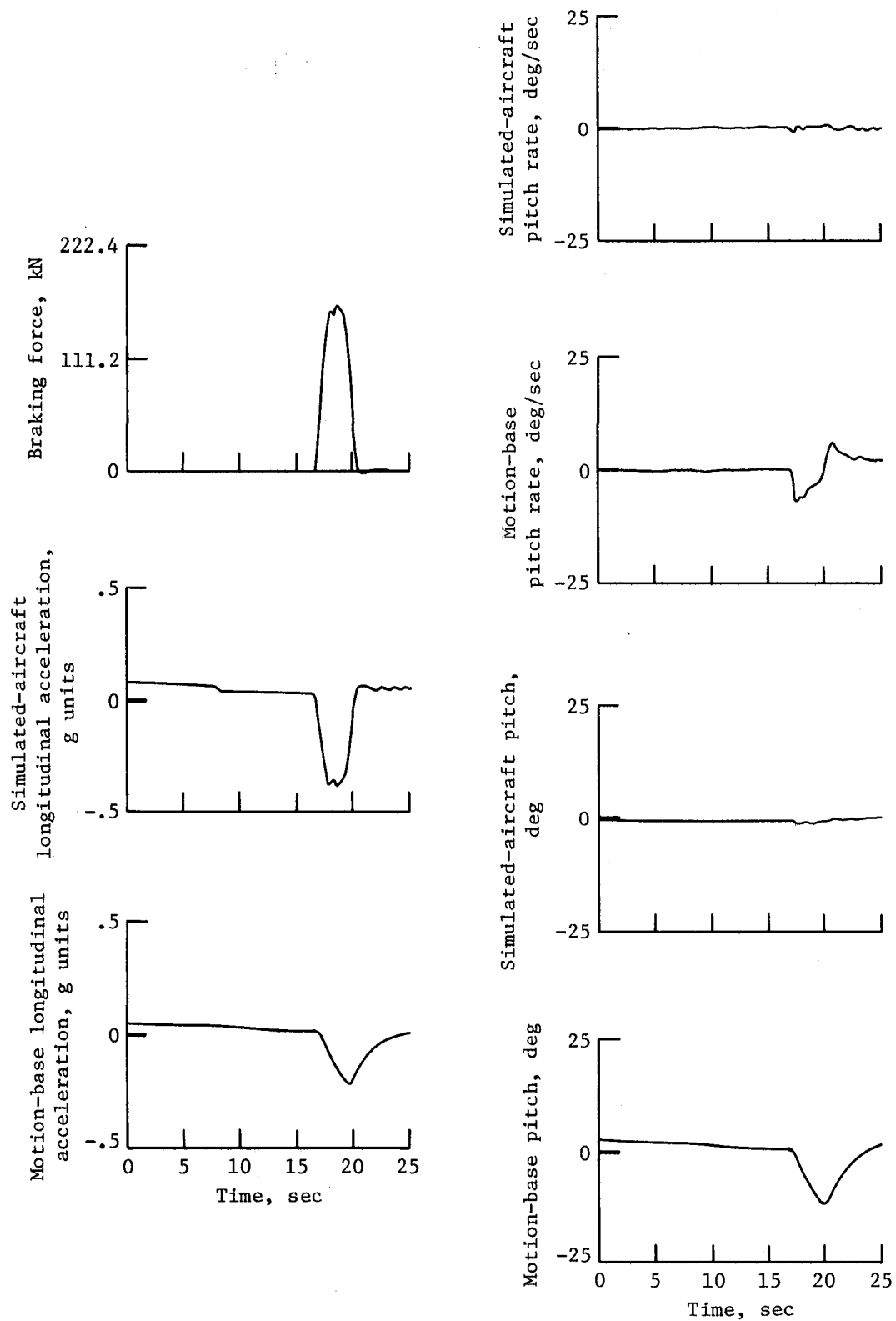


Figure 9.- Illustration of filtered braking-force application.

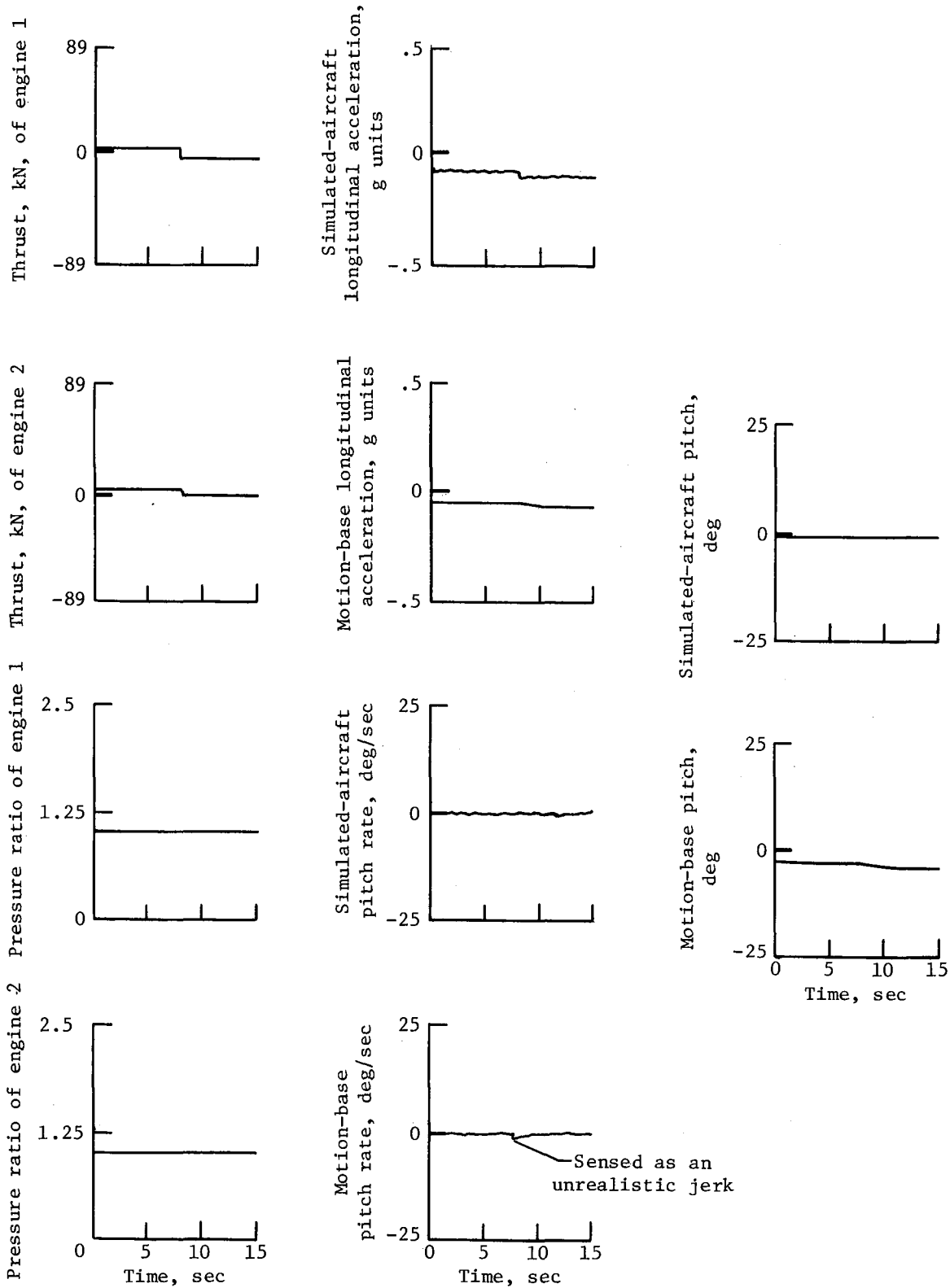
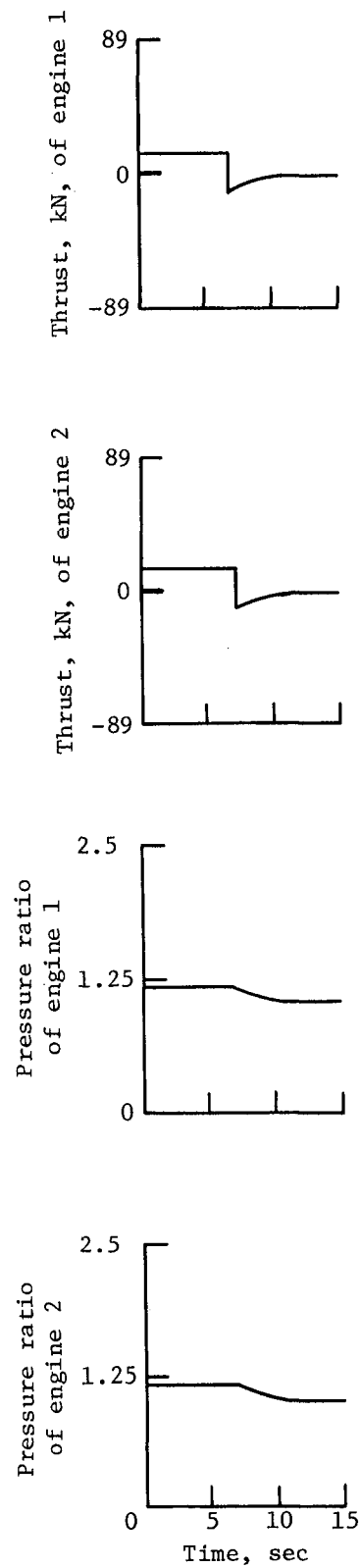
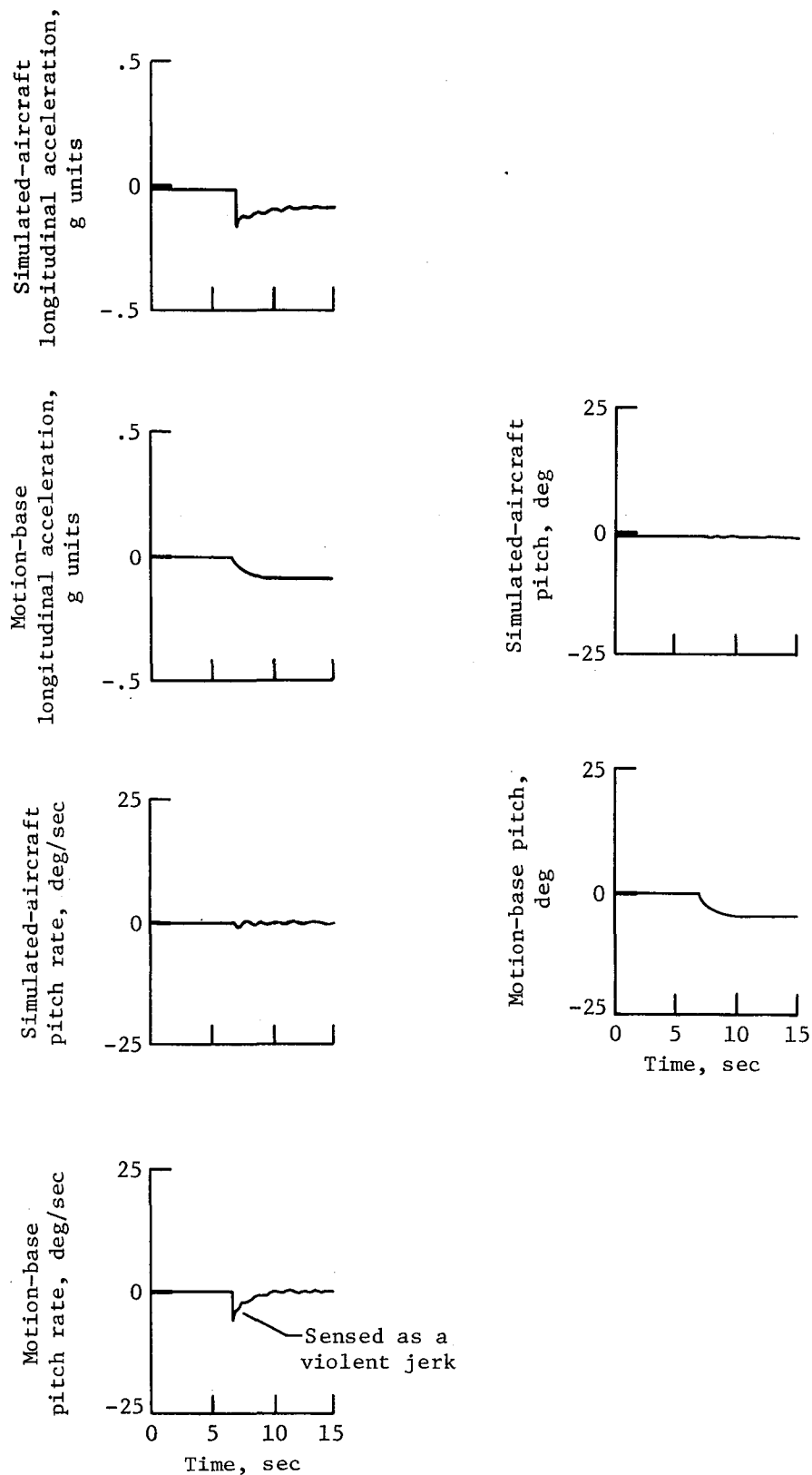


Figure 10.- Instantaneous change from positive to negative idle thrust.



(a) Individual engine time histories.

Figure 11.- Instantaneous change from high positive thrust to negative idle thrust.



(b) Acceleration, rate, and position time histories.

Figure 11.- Concluded.

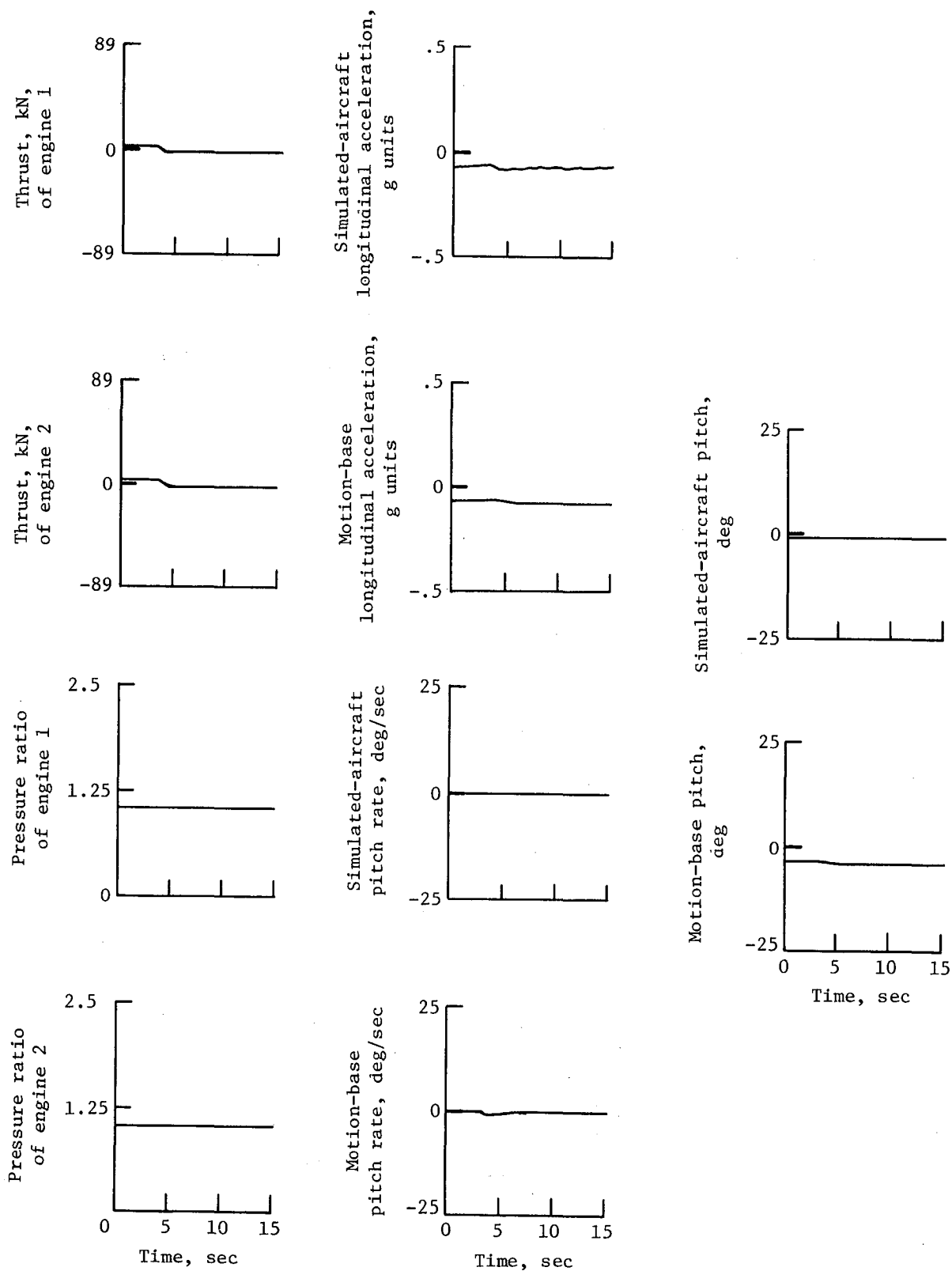
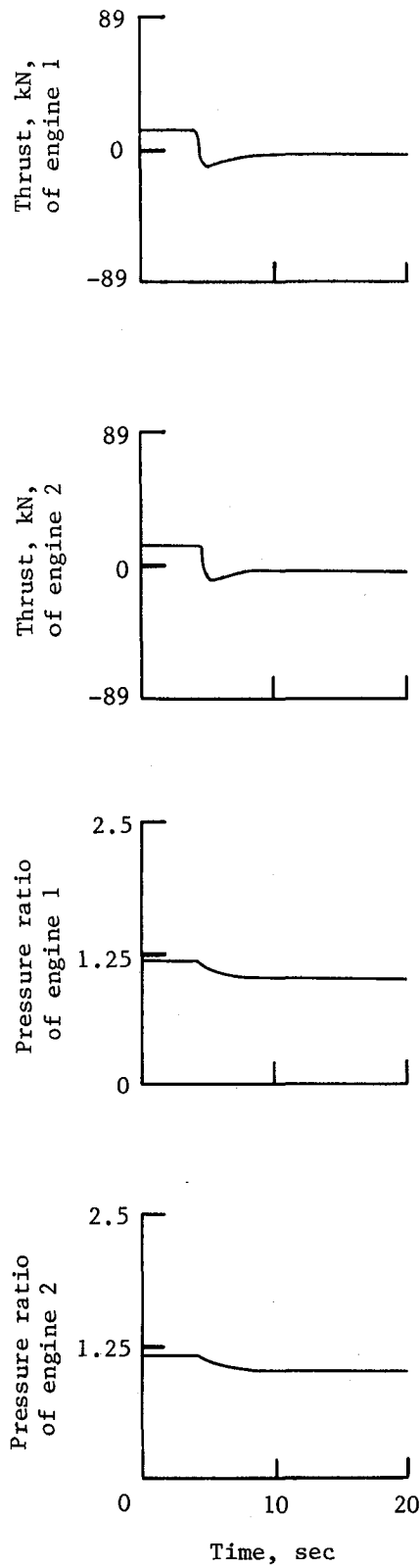
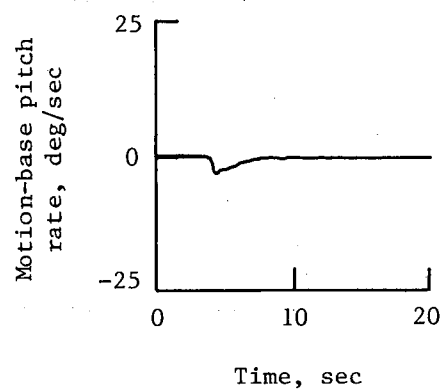
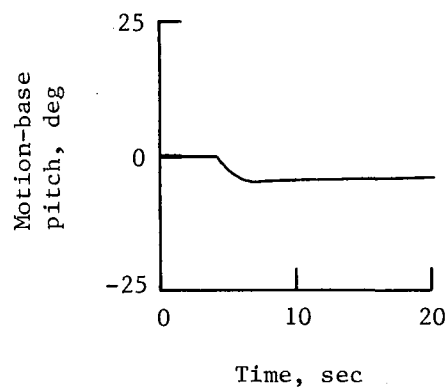
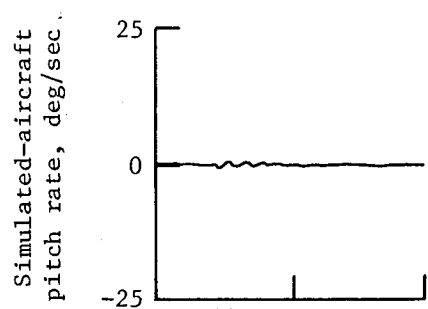
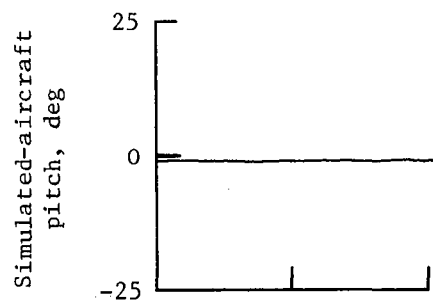
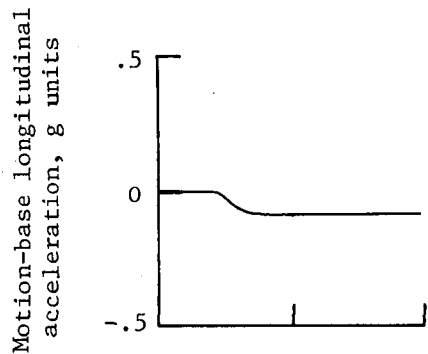
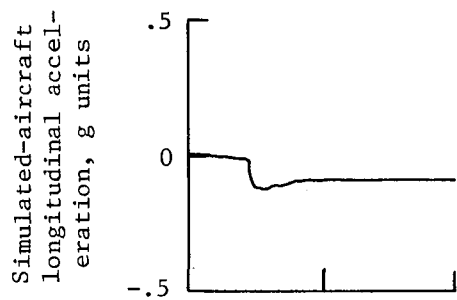


Figure 12.- Filtered change from positive to negative idle thrust.



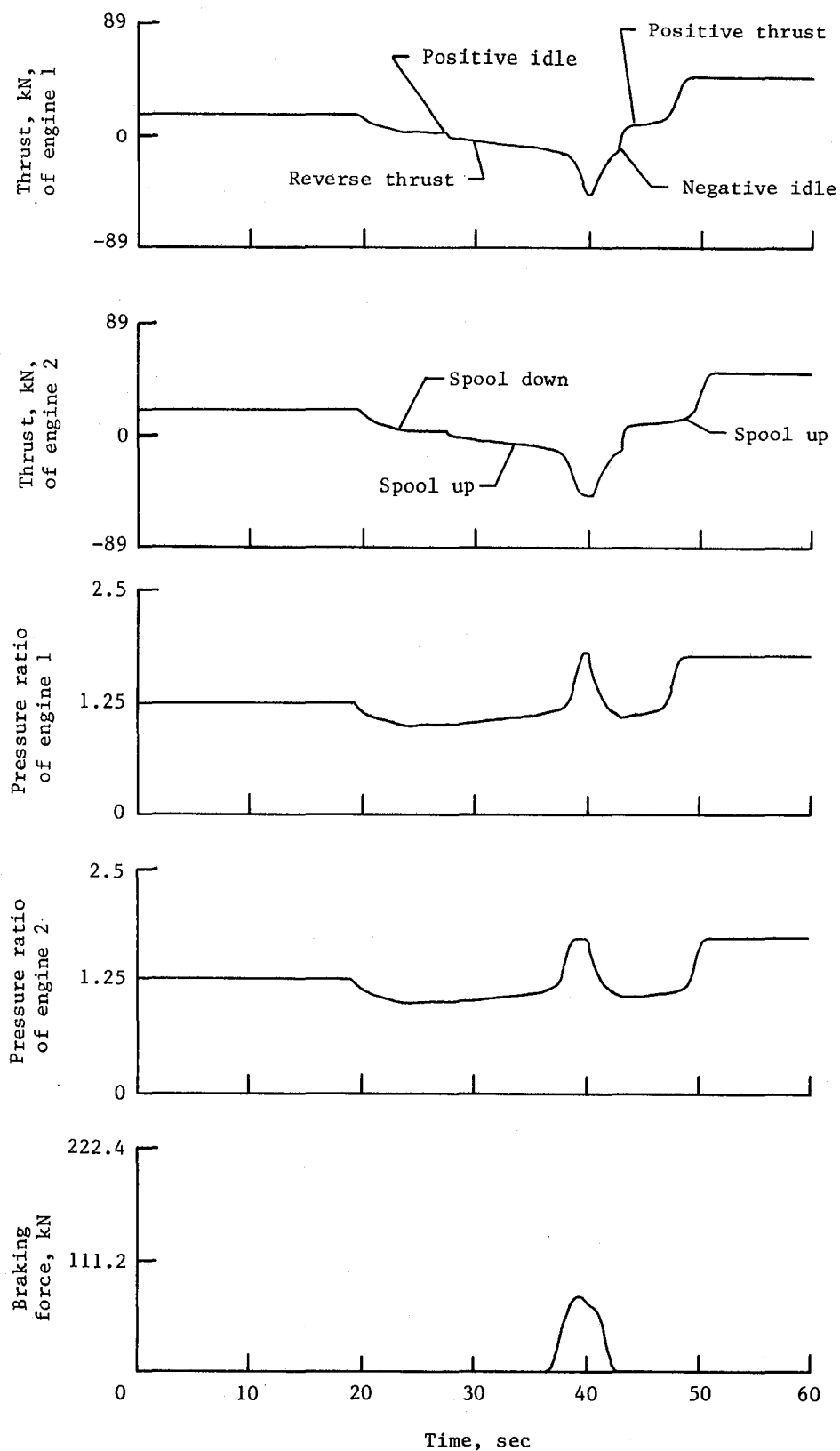
(a) Individual engine time histories.

Figure 13.- Filtered change from high positive thrust to negative idle thrust.



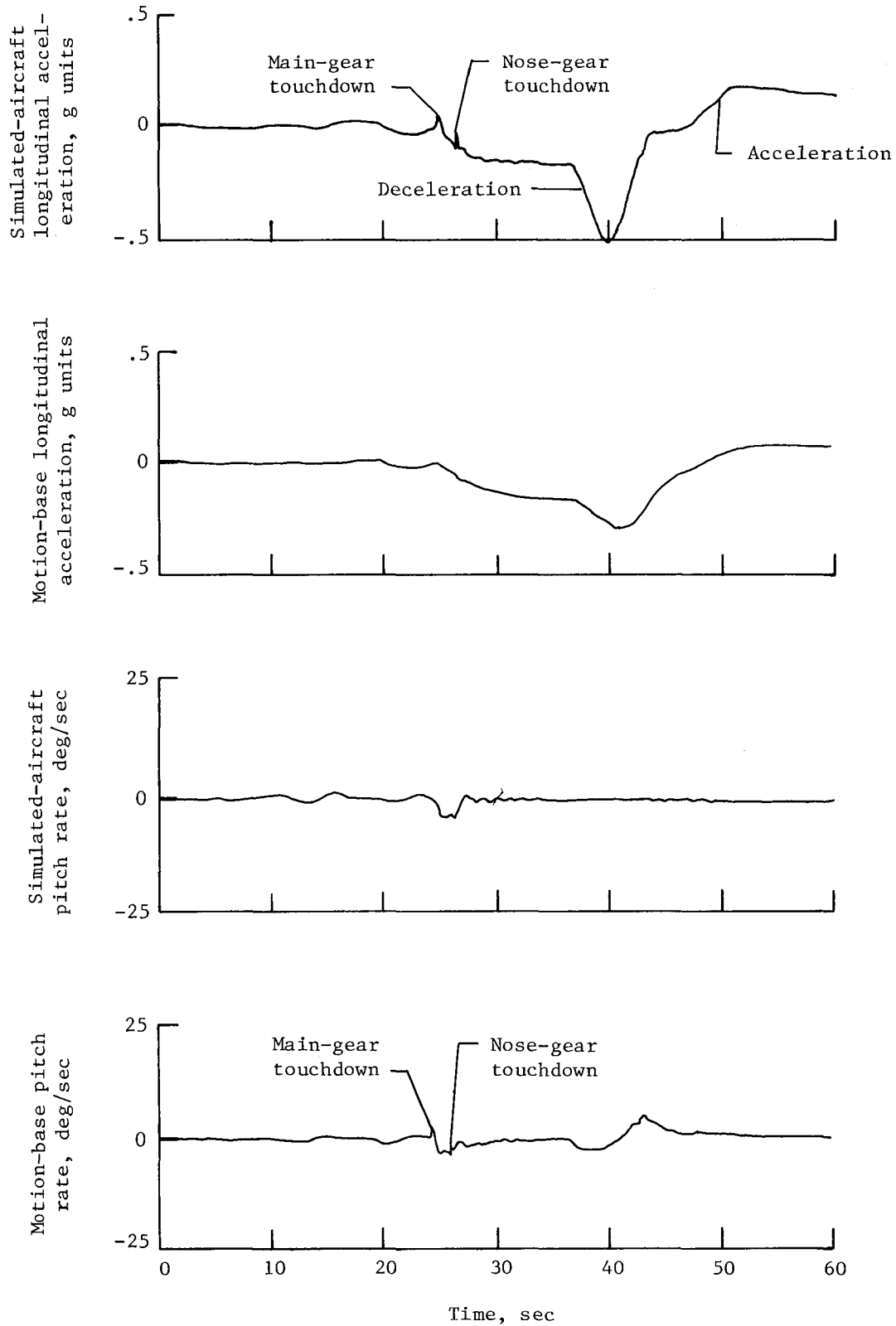
(b) Acceleration, rate, and position time histories.

Figure 13.- Concluded.



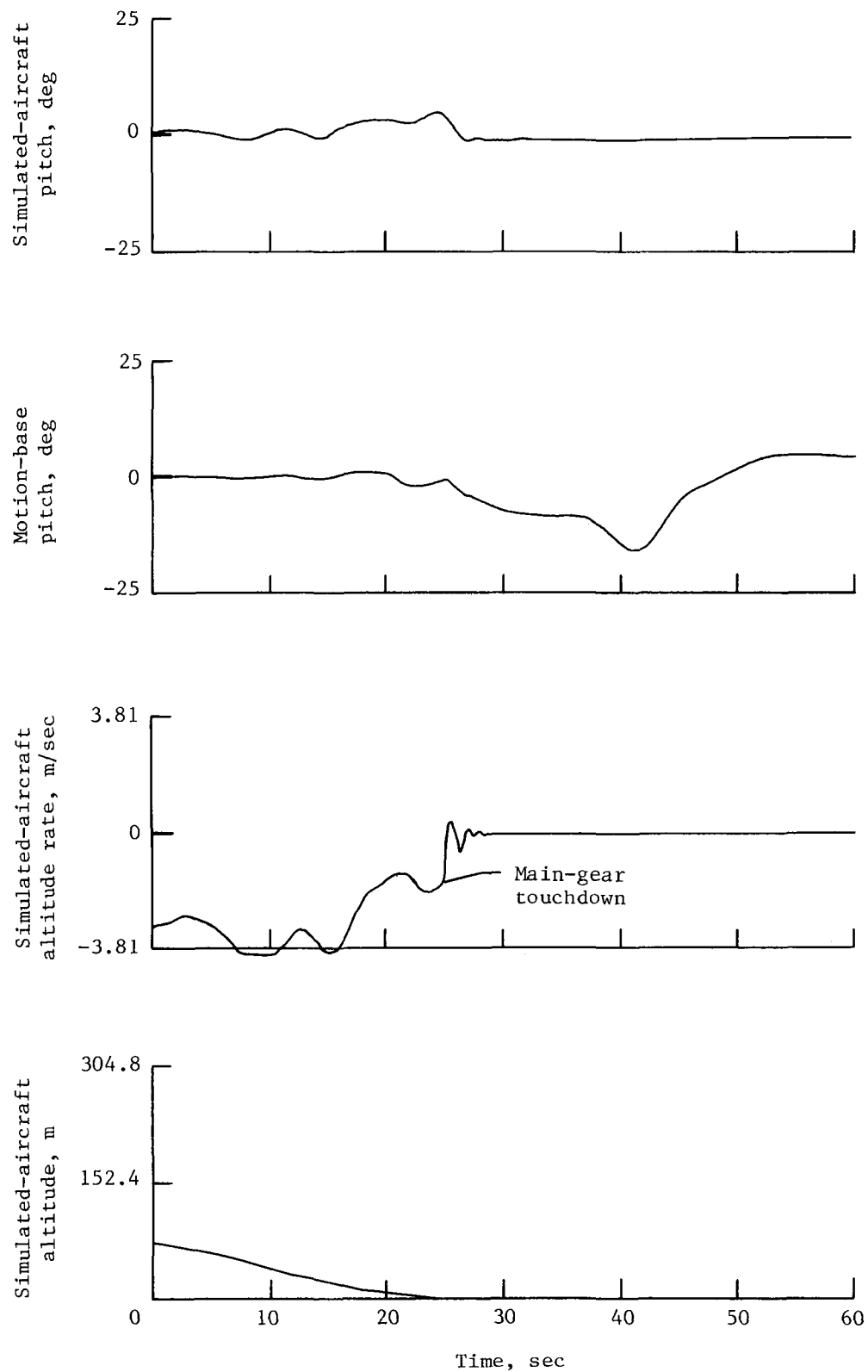
(a) Engine and braking time histories.

Figure 14.- Typical illustrations of touchdown, deceleration, and acceleration.



(b) Acceleration and rate time histories.

Figure 14.- Continued.



(c) Pitch angles, altitude rate, and altitude time histories.

Figure 14.- Concluded.

1. Report No. NASA TM-84568		2. Government Accession No.		3. Recipient's Catalog No.	
4. Title and Subtitle APPLICATION OF NONLINEAR ADAPTIVE MOTION WASHOUT TO TRANSPORT GROUND-HANDLING SIMULATION				5. Report Date February 1983	
				6. Performing Organization Code 505-35-33-01	
7. Author(s) Russell V. Parrish and Dennis J. Martin, Jr.				8. Performing Organization Report No. L-15530	
				10. Work Unit No.	
9. Performing Organization Name and Address NASA Langley Research Center Hampton, VA 23665				11. Contract or Grant No.	
				13. Type of Report and Period Covered Technical Memorandum	
12. Sponsoring Agency Name and Address National Aeronautics and Space Administration Washington, DC 20546				14. Sponsoring Agency Code	
15. Supplementary Notes Russell V. Parrish: Langley Research Center. Dennis J. Martin, Jr.: Sperry Systems Management, Hampton, Virginia.					
16. Abstract The application of a nonlinear coordinated adaptive motion washout to the transport ground-handling environment is documented. Additions to both the aircraft math model and the motion washout system are discussed. The additions to the simulated-aircraft math model provided improved modeling fidelity for braking and reverse-thrust application, and the additions to the motion-base washout system allowed transition from the desired flight parameters to the less restrictive ground parameters of the washout.					
17. Key Words (Suggested by Author(s)) Motion washout Nonlinear washout Ground handling Transport simulation Motion simulation				18. Distribution Statement Unclassified - Unlimited Subject Category 05	
19. Security Classif. (of this report) Unclassified	20. Security Classif. (of this page) Unclassified	21. No. of Pages 39	22. Price A03		

National Aeronautics and
Space Administration

Washington, D.C.
20546

Official Business

Penalty for Private Use, \$300

THIRD-CLASS BULK RATE

Postage and Fees Paid
National Aeronautics and
Space Administration
NASA-451



NASA

POSTMASTER: If Undeliverable (Section 158
Postal Manual) Do Not Return
